Overexpression of the epidermis-specific homeodomain-leucine zipper IV transcription factor OUTER CELL LAYER1 in maize identifies target genes involved in lipid metabolism and cuticle biosynthesis

Marie Javelle, Vanessa Vernoud, Nathalie Depège-Fargeix, Christine C. Arnould, Delphine Oursel, Frederic Domergue, Xavier Sarda, Peter Rogowsky

Overexpression of the Epidermis-Specific Homeodomain-Leucine Zipper IV Transcription Factor OUTER CELL LAYER1 in Maize Identifies Target Genes Involved in Lipid Metabolism and Cuticle Biosynthesis[1][C][W]

Marie Javelle[2], Vanessa Vernoud, Nathalie Depège-Fargeix, Christine Arnould, Delphine Oursel, Frédéric Domergue, Xavier Sarda, and Peter M. Rogowsky*

Université de Lyon, Ecole Normale Supérieure de Lyon, Université Lyon 1, Institut Fédératif de Recherche 128 BioSciences Lyon Gerland, Unité Reproduction et Développement des Plantes, F–69364 Lyon, France (M.J., V.V., N.D.-F., P.M.R.); INRA, UMR879 Reproduction et Développement des Plantes, F–69364 Lyon, France (M.J., V.V., N.D.-F., P.M.R.); CNRS, UMR5667 Reproduction et Développement des Plantes, F–69364 Lyon, France (M.J., V.V., N.D.-F., P.M.R.); Centre de Microscopie INRA/Université de Bourgogne, INRA, Centre de Microbiologie du Sol et de l'Environnement, F–21065 Dijon, France (C.A.); Laboratoire de Biogenèse Membranaire, Université Bordeaux II, CNRS-UMR5200, F–33076 Bordeaux, France (D.O., F.D.); and Biogemma, Laboratoire de Biologie Cellulaire et Moléculaire, F–63028 Clermont-Ferrand, France (X.S.)

Transcription factors of the homeodomain-leucine zipper IV (HD-ZIP IV) family play crucial roles in epidermis-related processes. To gain further insight into the molecular function of OUTER CELL LAYER1 (OCL1), 14 target genes up- or down-regulated in transgenic maize (*Zea mays*) plants overexpressing *OCL1* were identified. The 14 genes all showed partial coexpression with *OCL1* in maize organs, and several of them shared preferential expression in the epidermis with *OCL1*. They encoded proteins involved in lipid metabolism, defense, envelope-related functions, or cuticle biosynthesis and include *ZmWBC11a* (for white brown complex 11a), an ortholog of *AtWBC11* involved in the transport of wax and cutin molecules. In support of the annotations, *OCL1*-overexpressing plants showed quantitative and qualitative changes of cuticular wax compounds in comparison with wild-type plants. An increase in C24 to C28 alcohols was correlated with the transcriptional up-regulation of *ZmFAR1*, coding for a fatty acyl-coenzyme A reductase. Transcriptional activation of *ZmWBC11a* by OCL1 was likely direct, since transactivation in transiently transformed maize kernels was abolished by a deletion of the activation domain in OCL1 or mutations in the L1 box, a cis-element bound by HD-ZIP IV transcription factors. Our data demonstrate that, in addition to AP2/EREBP and MYB-type transcription factors, members of the HD-ZIP IV family contribute to the transcriptional regulation of genes involved in cuticle biosynthesis.

The outer-most cell layer or epidermis represents the interface of sessile land plants with their environment and has the somewhat incompatible roles to provide a protective barrier against hostile biotic or abiotic agents and at the same time to allow the exchange of gas, water, and nutrients with the outside world. The bulk of plant organs are covered by ground epidermal cells such as pavement cells on leaves or rhizodermic cells in the root. They show a certain asymmetry in that the cell wall facing the environment is frequently modified or reinforced (Glover, 2000). In addition, some epidermal cells undergo particular developments to form specialized structures such as trichomes or stomatal guard cells on the aerial parts, root hairs in the root, or the aleurone layer in the seed, which are essential for defense, respiration, nutrition, and starch degradation, respectively (Guimil and Dunand, 2007). Over the past few years, a wealth of knowledge has become available on the differentiation of these specialized epidermal cells, highlighting the importance of cell-cell communication, cell lineage, and the formation of particular transcriptional complexes in triggering specialization (Ishida et al., 2008; Nadeau, 2009). In contrast, little is known about the differentiation of ground epidermal cells. An impor-

[1] This work was supported by the Génoplante projects Maize TF (grant no. GABI–GP 2003–6) and MaizeYield (grant no. ANR–05–GPLA–031) and by the French Ministry of Higher Education (Ph.D. fellowship to M.J.).

[2] Present address: Cold Spring Harbor Laboratory, 1 Bungtown Road, Cold Spring Harbor, NY 11724.

* Corresponding author; e-mail peter.rogowsky@ens-lyon.fr.

The author responsible for distribution of materials integral to the findings presented in this article in accordance with the policy described in the Instructions for Authors (www.plantphysiol.org) is: Peter M. Rogowsky (peter.rogowsky@ens-lyon.fr).

[C] Some figures in this article are displayed in color online but in black and white in the print edition.

[W] The online version of this article contains Web-only data.

www.plantphysiol.org/cgi/doi/10.1104/pp.109.150540

tant step forward was the analysis of the shoot epidermal transcriptome in maize (*Zea mays*) and Arabidopsis (*Arabidopsis thaliana*) that highlighted the preponderant role of lipid-related functions in the epidermis. Indeed, genes involved in lipid metabolism, cuticle biosynthesis, or biotic/abiotic stress resistance were more abundantly expressed in shoot epidermal cells than in underlying tissues (Nakazono et al., 2003; Suh et al., 2005).

The control of the differentiation and maintenance of epidermal cell fate involves members of the homeodomain-Leu zipper IV (HD-ZIP IV) family of plant-specific transcription factors (Ariel et al., 2007). These proteins are defined by the presence of four highly conserved domains: a homeodomain (HD) associated with a Leu zipper domain (ZIP), a steroidogenic acute regulatory-related lipid transfer domain (START), and a HD-START-associated domain (Mukherjee and Burglin, 2006). The vast majority of characterized *HD-ZIP IV* genes have an epidermis-specific expression pattern in a variety of species, including Arabidopsis (Lu et al., 1996; Nakamura et al., 2006), cotton (*Gossypium hirsutum*; Guan et al., 2008), maize (Ingram et al., 2000), rice (*Oryza sativa*; Ito et al., 2002), and pine tree (*Pinus* spp.; Ingouff et al., 2001). Functional data concern almost exclusively the 16 *HD-ZIP IV* genes identified in the Arabidopsis genome (Nakamura et al., 2006), even though a systematic survey of single mutants revealed detectable phenotypes for only three of them. The *glabra2* (*gl2*) mutant is affected in trichome and root hair development, mucilage deposition, and seed oil content (Rerie et al., 1994; Di Cristina et al., 1996; Shen et al., 2006), the *homeodomain glabrous11* (*hdg11*) mutant in trichome branching (Nakamura et al., 2006), and the *anthocyaninless2* (*anl2*) mutant in anthocyanin distribution and root development (Kubo et al., 1999). A more spectacular phenotype was observed in the *Arabidopsis thaliana meristem layer1/protodermal factor2* (*atml1/pdf2*) double mutant, which fails to differentiate a protoderm during embryogenesis and is embryo lethal (Abe et al., 2003). Little is known about HD-ZIP IV target genes, and only four direct target genes have been identified. *PDF1*, a gene coding for a Pro-rich protein, is directly regulated by ATML1/PDF2 (Abe et al., 2003), and genes coding for the phospholipase D AtPLDζ1, the cellulose synthase CESA5, and the xyloglucan endotransglucosylase XTH17 are directly regulated by GL2 (Ohashi et al., 2003; Tominaga-Wada et al., 2009). The binding of the HD-ZIP IV proteins to these target gene promoters occurs at an 8-bp cis-element called the L1 box, which is thought to be critical for driving epidermis-specific expression (Abe et al., 2001).

In maize, five of the 17 *OUTER CELL LAYER* (*OCL*) genes encoding HD-ZIP IV proteins have been characterized and show an expression pattern restricted to the epidermal or subepidermal layer of various organs (Ingram et al., 2000). Functional data exist for *OCL4* involved in anther and trichome development (Vernoud et al., 2009) and *OCL1*. Dominant negative transgenic lines expressing an OCL1-ENGRAILED fusion show a transient reduction in kernel size, which is possibly caused by a decrease of gibberellin levels (Khaled et al., 2005).

In addition to Arabidopsis and maize, functional data are available in tomato (*Solanum lycopersicum*), where *CUTIN DEFICIENT2* (*CD2*) is necessary for the biosynthesis of an intact cuticle of the fruit (Isaacson et al., 2009). The cuticle is a protective hydrophobic layer deposited on the external cell wall of epidermal cells in the aerial parts of the plant (Jeffree, 2006). The two major constituents are cutin and waxes. The cutin polymer, a polyester of C16 to C18 fatty acids, represents the structural matrix, which is interspersed and covered by waxes, a mixture of C24 to C34 alcohols, aldehydes, fatty acids, alkanes, ketones, and wax esters (Jenks et al., 2002; Nawrath, 2002; Kunst and Samuels, 2003). Beyond its role in defense (Eigenbrode and Espelie, 1995), and more generally as a mechanical and chemical barrier against biotic and abiotic stress, the plant cuticle is also an efficient means against water loss and sun radiation and allows the control of gas exchanges (Gray et al., 2000; Riederer, 2006). Over the past few years, genetic studies in Arabidopsis have improved our understanding of the enzymatic steps involved in fatty acid elongation and wax biosynthesis (Samuels et al., 2008). In contrast, the mechanisms behind the transport and asymmetric deposition of cuticle components remain poorly understood. For over a decade, many authors hypothesized on the implication of lipid transfer proteins (LTPs) in the transport of cuticular lipids through the cell wall (Kader, 1996). A role of LTPs in cuticle formation has recently been demonstrated by the characterization of mutant Arabidopsis lines lacking LTPG1, which revealed a significant reduction of C29 alkanes in the cuticle (Debono et al., 2009; Lee et al., 2009). Beyond LTPs, there is experimental evidence that the ATP-binding cassette (ABC) transporters ABCG12/CER5 (for ECERIFERUM5) and ABCG11/WBC11 (for WHITE BROWN COMPLEX11) are involved in the transport of wax (CER5) or wax and cutin molecules (WBC11) from their site of synthesis to the cuticle layer (Pighin et al., 2004; Bird et al., 2007).

Here, we provide evidence for a link between the HD-ZIP IV transcription factor OCL1 from maize and certain elements of lipid transport/metabolism, in particular elements needed for cuticle deposition/biosynthesis necessary to make a protective epidermis. We identified 14 direct or indirect target genes of OCL1 and show that the transcriptional activation by OCL1 of a gene coding for an ABC transporter is likely direct and involves an L1 box.

RESULTS

Identification of 11 OCL1 Target Genes by Microarray Analysis

Eleven target genes of the HD-ZIP IV transcription factor OCL1 were identified by a transcriptome com-

parison between transgenic maize plants overexpressing OCL1 (*OCL1*-OE) under the control of the strong cassava vein mosaic virus (CsVMV) promoter and wild-type sister plants. RNA was extracted from the aerial parts of plantlets at 18 d after sowing (DAS) and used to hybridize a genome-wide 59 K microarray. A first gene list of 204 differentially expressed genes was established based on $P < 0.01$ for the biological triplicate and strong expression differences ($\log R > 2$ or < -2). Using a medium to high spot intensity ($\log I > 0$) as an additional criterion, the list was shortened to 35 candidates. The differential expression was confirmed for 11 of the 35 candidate genes by quantitative reverse transcription (qRT)-PCR experiments based on the same samples that had been used for the initial microarray analysis (Table I; Supplemental Table S1).

A survey of two additional organs suggested that OCL1 was not the only regulatory protein influencing the transcription of its target genes and/or that it might interact with different proteins or via different regulatory cascades in dissected shoot apices and in immature ears. Three target genes (MZ00014373, MZ00024305, and MZ00031955) had the same differential trend in all three organs, while in seven other cases the trend was confirmed only in two of the three organs and in one case only in the original 18-DAS plantlets (Table I). Expression differences between *OCL1*-OE and the wild type were generally lower in the additional organs, reflecting lower ratios for *OCL1* itself, which were probably caused by less efficient transcription off the CsVMV promoter in shoot apices and immature ears. Taken together, we identified 11 genes that were either directly or indirectly up-regulated (six genes) or down-regulated (five genes) by OCL1.

Involvement of OCL1 Target Genes in Lipid Metabolism, Lipid Transfer, and/or Plant Defense

To determine whether the 11 confirmed target genes had similar functions, complete protein sequences were assembled, starting from the 70-nucleotide oligonucleotide deposited on the microarray, exploiting the very rich maize EST data (Messing and Dooner, 2006) as well as the recently established draft of the maize genome sequence (Pennisi, 2008). A group of five genes shared annotations related to lipid metabolism or transport and/or plant defense (Table I). Among them, three up-regulated target genes likely encoded lipid transporters, as they were annotated as nonspecific, type 2 lipid transfer protein (MZ00024305; hereafter named ZmLTPII.12 according to Boutrot et al. [2008]), ABC transporter of the WBC11/ABCG11 clade (MZ00031783), and SEC14/phosphatidylinositol transfer protein (MZ00031955, PITP). Another up-regulated gene (MZ00029574) shared highest identity with *AtCXE18* encoding an Arabidopsis carboxylesterase hydrolyzing in vitro short-chain acyl esters (Cummins et al., 2007). Finally, the down-regulated (MZ00005958) *Indole-3-glycerol phosphate lyase* (*Igl*) gene had previously been shown to be involved in the tritrophic defense of maize against herbivory (Frey et al., 2000). While a sixth gene (MZ00018561) also carried a plant lipid transfer protein domain, its N-terminal extension made it an atypical LTP and led to a classification as a Pro-rich cell wall-plasma membrane linker protein with lipid-binding capacity. Two other target genes also seemed to have a cell envelope-related function due to their annotations as transmembrane proteins, and more precisely, members of a plant-specific family carrying the DUF588 domain (for domain of unknown function 588; MZ00030315) and of the MtN3/Saliva family (MZ00014373) named after NODULIN3 from *Medicago truncatula* and SALIVA from *Drosophila melanogaster* (Gamas et al., 1996). This group was completed by a down-regulated gene (MZ00024414) annotated as a multidrug and toxic compound extrusion (MATE) efflux carrier. The last two genes were predicted to encode a cytochrome P450 of the plant-specific subfamily A most closely related to CYP78A6 from Arabidopsis and a tetratricopeptide repeat (TPR) domain-containing protein similar to the MALE STERILITY5 protein (Glover, 2000). These results suggested that the majority of genes regulated by OCL1 were involved in lipid metabolism or transport and other cell envelope-related functions.

Due to the epidermis-specific expression of *OCL1*, we scrutinized the 11 annotations for putative epidermis-related functions. In the case of the *WBC11*-like gene (MZ00031783), which will be called *ZmWBC11a* hereafter, functional data in a closely related gene clearly suggested an epidermis-related function, since both wax and cutin synthesis are impaired in the Arabidopsis *wbc11* mutant (Bird et al., 2007). In order to determine if OCL1 regulated other members of the WBC11 clade in maize, we identified all paralogous genes in the maize genome. Among the four additional *WBC11*-like genes, *ZmWBC11b* to *ZmWBC11e*, the first two showed up-regulation in transgenic 18-DAS plantlets compared with wild-type plantlets (Table I). Interestingly, the three *ZmWBC11* genes regulated by OCL1 (*ZmWBC11a*, *ZmWBC11b*, and *ZmWBC11c*) fell into a single clade in the phylogenetic tree of the WBC family, while the remaining two genes, *ZmWBC11d* and *ZmWBC11e*, not influenced by OCL1 fell into a sister clade (Supplemental Fig. S1). These results indicated that OCL1 regulated a well-defined subset of genes coding for ABC transporters in maize.

Overlapping Expression of *OCL1* with Its Target Genes

To obtain additional clues with regard to gene function, we established the expression pattern of each confirmed target gene by qRT-PCR in vegetative and reproductive organs as well as during kernel development (Fig. 1; Supplemental Table S2). Three genes of the lipid group (*ZmLtpII.12*, *ZmWBC11a*, and MZ0031955) and one of the envelope group (MZ00018561) showed

Table I. *Relative expression levels of confirmed OCL1 target genes in OCL1-OE and OCL1-RNAi plants*

Oligo ID[a] and/or Gene Name	Trend in *OCL1*-OE (Plantlet)	Ratio *OCL1*-OE/ Wild Type[b]			Ratio *OCL1*-RNAi/ Wild Type[c]	Annotation[f]	Maize Gene Model[g]	Class
		18-DAS Plantlet	Shoot Apex[d]	Immature Ear[d]	18-DAS Plantlet[e]			
OCL1	Up	23.80	4.00*	3.46*	0.51*	Transcription factor HD-ZIP IV family	GRMZM2G026643	Transcription factor
MZ00005958	Down	0.18	1.50	0.00*	1.38*	Maize indole-3-glycerol phosphate lyase (Igl)	GRMZM2G015892	Defense
MZ00014373	Down	0.10	0.39*	0.04*	1.05	MtN3/SALIVA-related transmembrane protein	GRMZM2G179349	Envelope
MZ00018561	Down	0.38	0.57*	1.87	0.99	Pro-rich protein; structural constituent of cell wall	GRMZM2G345700	Envelope
MZ00022171	Up	20.88	0.43	0.43	1.04	Male sterility MS5 family protein; contains TPR domain	GRMZM2G075563	Other
MZ00024305 *LtpII.12*	Up	4.34	1.94*	2.40*	0.58*	Nonspecific lipid transfer protein (nsLTP) type 2	GRMZM2G387360	Lipid
MZ00024414	Down	0.09	0.65*	1.52	1.23*	MATE efflux family protein	GRMZM2G339488	Envelope
MZ00028617	Down	0.04	0.61*	1.61	1.30*	Cytochrome P450; oxygen binding; CYP78A6-like	GRMZM2G034471	Other
MZ00029574	Up	7.35	1.25*	nd	0.80*	Carboxylesterase; ATCXE18-like	GRMZM2G104141	Lipid
MZ00030315	Up	13.51	1.55*	0.18	0.55*	Integral membrane family protein; contains DUF588	GRMZM2G132128	Envelope
MZ00031783 *ZmWBC11a*	Up	6.94	1.05	1.27*	0.73*	ABC transporter; ABCG11/ COF1/DSO/WBC11-like	GRMZM2G308860	Lipid
MZ00031955	Up	7.08	2.57*	2.17*	1.09	SEC14/phosphoglyceride transfer family protein	GRMZM2G088501	Lipid
ZmFAR1	Up	2.78	nd	nd	1.21	Fatty acyl-CoA reductase (alcohol-forming)/ oxidoreductase; FAR1-like	GRMZM2G036217	Lipid
ZmWBC11b	Up	2.69	nd	nd	1.00	ABC transporter; ABCG11/ COF1/DSO/WBC11-like	GRMZM2G096952	Lipid
ZmWBC11c	Up	2.06	nd	nd	0.49*	ABC transporter; ABCG11/ COF1/DSO/WBC11-like	GRMZM2G143668	Lipid

[a]Identification number of the corresponding oligonucleotide deposited on the microarray. [b]Mean of a biological triplicate and a technical replicate; the expression values are reported relative to one of the wild-type samples. [c]Mean of a technical triplicate; the expression values are reported relative to the wild-type samples. [d]Asterisks indicate a trend of differential expression similar to the one observed in *OCL1*-OE plantlets. nd, Not determined. [e]Asterisks indicate a trend of differential expression opposite to the one observed in *OCL1*-OE plantlets. [f]Manually improved annotations from SwissProt, GenBank, Trembl, and InterPro databases. [g]Maize genome release 4a.53 of March 8, 2010 (http://www.maizesequence.org).

strongest expression in reproductive organs, while the remaining three genes of the envelope group (MZ00014373, MZ00024414, and MZ00030315) and the *Cytochrome P450* gene (MZ00028617) were primarily expressed in leaves (Fig. 1). The fourth lipid gene (MZ00029574) and the defense gene (MZ00005958) showed no clear preference for either reproductive organs or leaves. The gene coding for a TPR domain protein (MZ00022171) appeared to be preferentially expressed in the maize kernel. During kernel development, the majority of the 11 target genes showed a peak of expression toward the end of early kernel development, varying between 7 and 12 d after pollination (DAP; Supplemental Table S2). One of the lipid-related genes (MZ00031955) had a second peak during the maturation stage (35–50 DAP). Expression of the *Nodulin* gene (MZ00014373) was strongest in immature ovules, while the *Cytochrome P450* gene (MZ00028617) was up-regulated during dehydration (30–35 DAP).

In conclusion, most genes clearly showed preferential expression in a limited number of organs. Despite preferences for either leaves or reproductive organs and generally weaker expression in roots, we could not establish an overall pattern common to all genes, although the expression territories of all genes showed at least some overlap with that of *OCL1*, in particular during kernel development.

Due to the annotations suggesting epidermis-related functions of the 11 target genes, we performed RT-PCR experiments on epidermal and mesophyll cells captured after laser microdissection of the central part of juvenile leaf 4 (Fig. 2A) in order to reveal any preferential or specific expression in the epidermis. Of

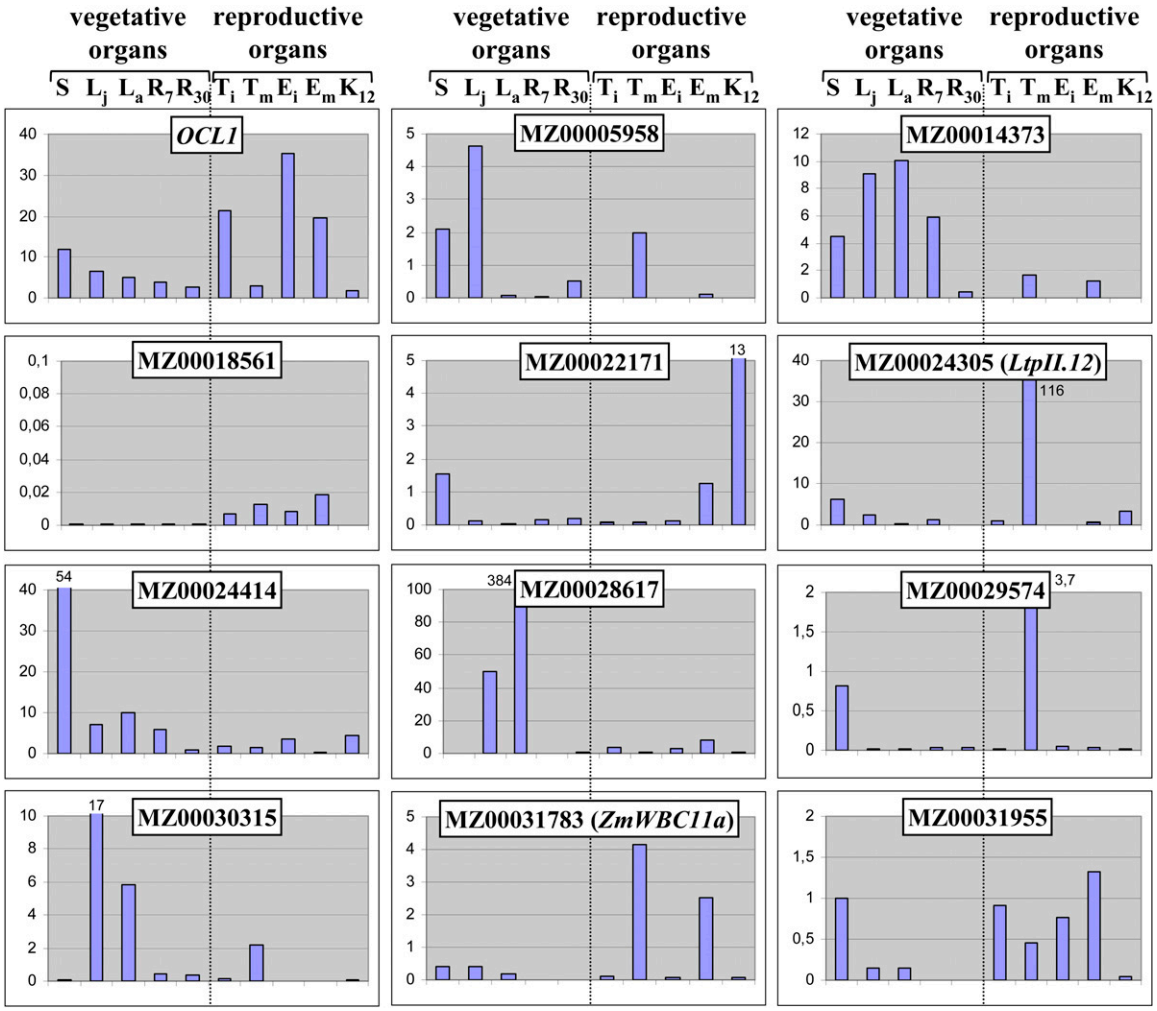

Figure 1. Expression profile of *OCL1* and its target genes in maize. Real-time RT-PCR experiments were carried out on cDNA prepared from major organs of the maize plant for *OCL1* and its 11 target genes identified by microarray experiments. The values are means of a technical replicate. The values of truncated bars are indicated. S, Seedling aerial parts; L_j, leaf juvenile (leaf 4); L_a, leaf adult (leaf 10); R_7, root at 7 DAS; R_{30}, root at 30 DAS; T_i, tassel immature; T_m, tassel mature; E_i, ear immature; E_m, ear mature; K_{12}, kernel at 12 DAP. [See online article for color version of this figure.]

the 11 target genes, *ZmLTPII.12* (MZ0024305) and the gene encoding a Pro-rich protein (MZ00018561) were specifically expressed in the epidermis, while *Igl* (MZ00005958) and the gene coding for an integral membrane protein (MZ00030315) showed preferential expression in this layer. Two genes were evenly expressed in both tissues (MZ00031955 and *ZmWBC11a*), four showed stronger or specific expression in mesophyll cells (MZ00014373, MZ00022171, MZ00024414, and MZ00028617), and one was not detectable in either tissue (MZ00029574). The expression of *OCL1* was only preferential but not specific to epidermal cells (Fig. 2), a situation reminiscent of the one observed by in situ hybridization in very young embryos but in contrast with in situ hybridizations on organ primordia or meristematic tissues suggesting epidermis-specific expression (Ingram et al., 1999). In summary, the data further strengthened the hypothesis of a role of *OCL1* and the first four genes in epidermis-related functions, but they do not exclude such a role for the remaining genes.

Changes in Cuticular Wax Composition in *OCL1*-OE Plants

Since the lipid-related target gene *ZmWBC11a* belonged to the same orthologous group as *AtWBC11*, which has a clearly established role in cuticle formation in Arabidopsis, we analyzed the leaves of transgenic lines overexpressing *OCL1* for structural modifications of the cuticle. The thickness of the cuticle was measured by transmission electron microscopy and confocal microscopy in transverse sections of juvenile leaves, while the density and shape of wax crystals were assessed by scanning electron microscopy. Neither approach revealed any significant

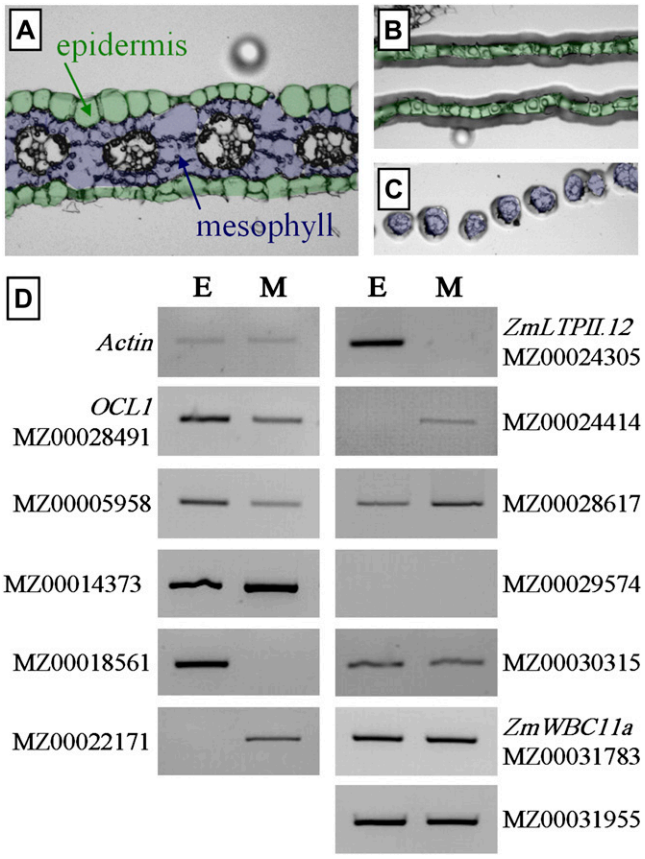

Figure 2. Expression of *OCL1* and its target genes in outer and inner cell layers of leaf 4. A to C, From paraffin-embedded leaf sections (A), epidermal (B) and mesophyll cells (C) were isolated using infrared laser-capture microdissection. D, RT-PCR experiments assessing the expression of OCL1 and its target genes in microdissected epidermal (E) and mesophyll (M) cells. The concentration of the cDNA templates was normalized according to the abundance of the *Actin* RT-PCR product. [See online article for color version of this figure.]

differences between wild-type and *OCL1*-OE leaves (Supplemental Fig. S2).

Next, we employed biochemical methods based on chloroform extraction followed by gas chromatography with flame ionization detection or mass spectrometry detection to analyze the quantity and quality of epicuticular waxes from juvenile leaves. Using juvenile leaf 4 from two independent *OCL1*-OE transformation events (K2 and K3) and their corresponding wild type, we analyzed waxes from both the leaf sheath (the leaf base enveloping the stem) and the leaf blade (the part separated from the stem). No significant difference could be detected in the total wax load for either part of the leaf, but a detailed analysis of the different constituents revealed that the same pools were affected in the two independent *OCL1*-OE lines (Fig. 3), which showed comparable levels of *OCL1* overexpression (19.57-fold for K2 and 23.80-fold for K3). In the leaf sheath, *OCL1* overexpression modified the content of the two major components of the waxes with opposite effect: increase in C32 alcohol and decrease in C32 aldehyde. Nevertheless, since these constituents were present at about the same levels and the modifications were similar but in opposite directions, total wax load was not affected. With respect to minor components, strong modifications were consistently detected in the levels of the wax esters, which are made of very long-chain fatty acids and alcohols. In the waxes of both *OCL1*-OE events, C44 to C48 wax esters were two to three times more abundant. In event K2, this increase in wax ester content was accompanied by higher levels of C26 fatty alcohol and C27 alkane. In the leaf blade, the contents of the two major components (C32 alcohol and C32 aldehyde) were not affected. Among the minor components, C46 and C48 wax esters were reduced (by approximately 30%) rather than increased as in the leaf sheath. Fatty alcohols showed a much broader increase, since the levels of C24 to C28 alcohols were about 30% higher in both *OCL1*-OE events when compared with the wild type. In addition, the levels of C25 alkane and C28 and C30 aldehyde (event K2 only) were significantly increased in the blade. Altogether, these analyses suggested that overexpression of *OCL1* resulted in significant modifications of wax composition, with somewhat different effects in sheath and blade.

Since in epicuticular waxes of Arabidopsis the production of primary alcohols is catalyzed by the fatty acyl-coenzyme A reductase (FAR) CER4 (Costaglioli et al., 2005; Rowland et al., 2006), we hypothesized that OCL1 could activate the transcription of *FAR* genes in maize leaf blades. Therefore, we identified the FARs present in the maize genome based on sequence homology to Arabidopsis FARs and examined their expression level in wild-type and *OCL1*-OE plants. Among the five putative *ZmFAR* genes detected in the maize genome, only *ZmFAR1* showed a differential expression and was up-regulated 2.78-fold in *OCL1*-OE plants (Table I). While reciprocal blast analyses revealed that the closest relatives of the deduced ZmFAR1 protein sequence in Arabidopsis were CER4 (At4g33790) and At5g22500, with 64% sequence identity each, phylogenetic analyses did not allow establishing orthologous relationships between individual proteins. Four maize sequences including ZmFAR1 were clustered in a clade, and six Arabidopsis sequences including CER4 were clustered in a sister clade (Supplemental Fig. S3). These results indicated that OCL1 may trigger the reduction of fatty acid precursors into primary alcohols through the transcriptional activation of a particular *ZmFAR* related to *AtCER4*.

Partial Knockouts of *OCL1* Influence Target Gene Expression But Not Wax Composition

To confirm the molecular and phenotypic changes seen in *OCL1*-OE plants, *OCL1*-RNAi (for RNA interference) plants under the control of the rice *Actin* promoter were produced. None of the 14 transforma-

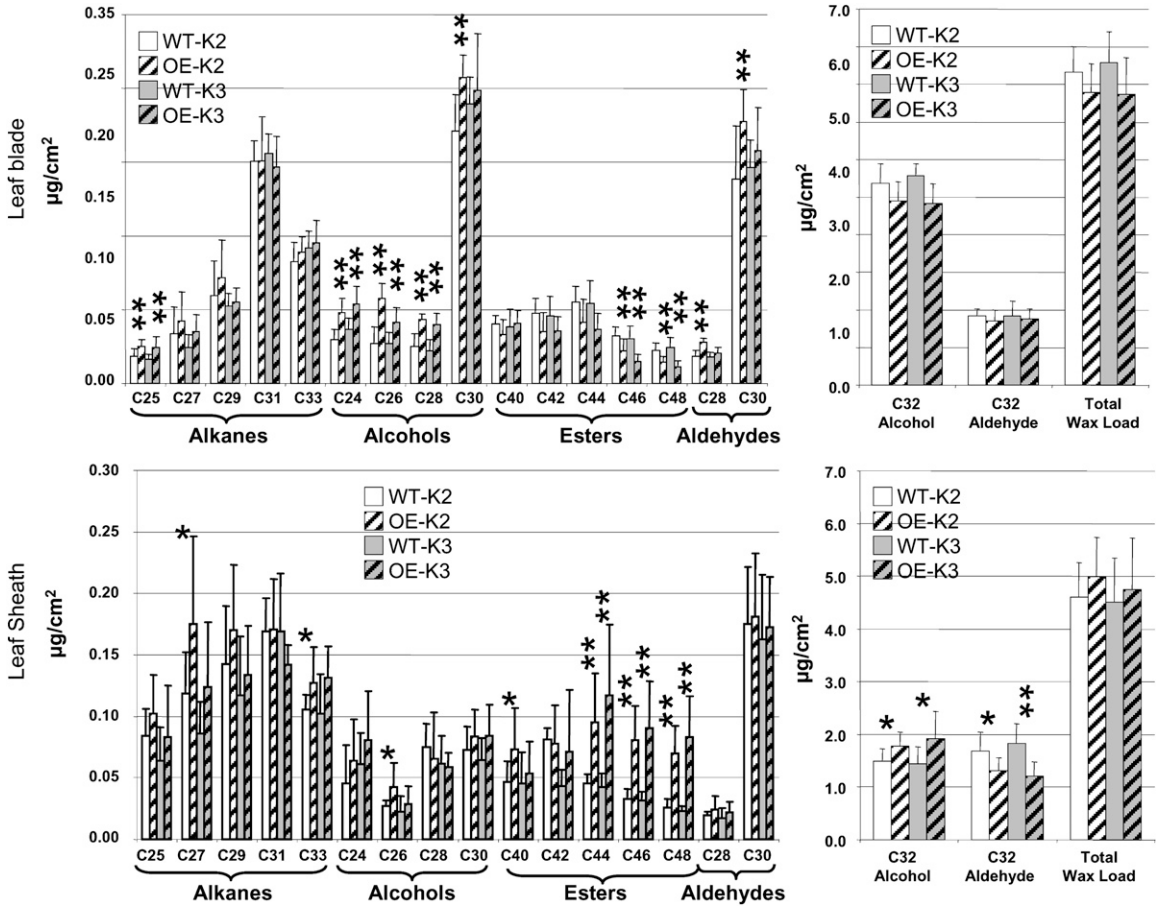

Figure 3. Cuticular wax composition of juvenile maize leaves. Total wax load as well as relative amounts of individual compounds from the blade and sheath of juvenile leaves were compared between the *OCL1*-OE transformation events K2 and K3 (hatched bars) and their respective wild types (WT; white and gray bars). Means and SD indicated by error bars were calculated on seven to 10 biological replicates (Supplemental Table S3). * $P < 0.05$, ** $P < 0.01$ as calculated by Student's *t* test.

tion events showed complete suppression of *OCL1* transcript accumulation, and further work focused on line 2, which showed the most efficient *OCL1* gene silencing, with a decrease of about 50% of the *OCL1* mRNA level (Table I). This knockdown of *OCL1* expression was sufficient to affect the expression level of several target genes. In 18-DAS plantlets, eight target genes had a trend opposite to the one observed in *OCL1*-OE plants (Table I). Again, the lipid group was the main representative, with the ABC transporter genes *ZmWBC11a*, *ZmWBC11c*, and *ZmLTPII.12* and the *Carboxylesterase* gene (MZ00029574). Five target genes showed no significant expression difference between *OCL1*-RNAi plantlets and wild-type siblings, and one gene showed the same trend as in *OCL1*-OE plants. These data lend further credence to a direct or indirect regulation by OCL1 of the eight genes, with opposite trends in *OCL1*-OE and *OCL1*-RNAi plantlets.

Wax composition was analyzed in three independent RNAi events named lines 1, 2, and 3, in which the *OCL1* expression level was reduced to 68%, 51%, and 64% of the wild-type level, respectively. A comparative analysis of juvenile leaves from RNAi plants and wild-type siblings revealed significant differences only for wax esters (Supplemental Table S3), which were somewhat difficult to interpret in light of the differences between sheath and blade. No opposite trend to the increase of C24 to C28 alcohols seen in *OCL1*-OE lines was observed, probably due to the insufficient knockdown of *OCL1*. In fact, opposite trends are not necessarily expected, since *OCL1* expression was only reduced by a factor of 2 in the best *OCL1*-RNAi line but increased by a factor of 20 in the strongest *OCL1*-OE line; similarly, the alterations in the expression of the eight target genes with opposite trends were considerably stronger in *OCL1*-OE lines than in the *OCL1*-RNAi line.

Transactivation of *ZmWBC11a* and *ZmLtpII.12* by OCL1 after Transient Transformation of Maize Kernels

In order to discriminate between direct and indirect OCL1 target genes, we obtained the genomic sequence

of each target gene using maize genome resources (www.maizegenome.org) and scanned the upstream and intron sequences for the presence of an L1 or L1-like (L1L) box. The asymmetric L1 box 5′-TAAATG (C/T)A-3′ is a cis-element showing a gel shift in the presence of the HD-ZIP IV transcription factors ATML1 (Abe et al., 2001), PDF2 (Abe et al., 2003), and GL2 (Ohashi et al., 2003), while the slightly longer palindromic L1L box 5′-GCATTAAATGC-3′ has been defined as the consensus-binding site of recombinant HD-ZIP IV proteins HDG7, HDG9, and ATML1 in PCR-assisted DNA selection assays (Nakamura et al., 2006). The only L1 or L1L box detected in the 11 genomic sequences was located near the end of the first intron of *ZmWBC11a* (Fig. 4), which became a good candidate to be a direct target gene of OCL1. The presence of regulatory elements in introns is not rare, one of the best characterized examples being intron 1 of *AGAMOUS* in Arabidopsis (Sieburth and Meyerowitz, 1997).

To further investigate the possible binding of OCL1 to regulatory regions of target genes, we chose the L1 box-containing intron of *ZmWBC11a* and the upstream region of the epidermis-specific *ZmLtpII.12* (Fig. 4A). Immature maize kernels were cobombarded with fusions of the respective regulatory regions to a *GUS* reporter gene and a second construct expressing *OCL1* under the control of the constitutive CsVMV promoter. Quantification of GUS activity by the 4-methylumbelliferyl β-D-glucuronide test revealed a basal level of fluorescence after transient transformation with the reporter constructs *iWBC11a*::*GUS* and *pLtpII.12*::*GUS* on their own (Fig. 4B). When cotransformed with *OCL1*, we observed a marked increase in GUS activity indicating transactivation by OCL1. In contrast, the cotransformation of *pLtpII.12*::*GUS* or *iWBC11a*::*GUS* with *OCL1ΔAD* coding for an inactive form of OCL1 lacking its activation domain (N. Depège-Fargeix, personal communication) failed to transactivate the transcription of the *ZmLtpII.12* and *ZmWBC11a* genes, and we even observed a weak, nonsignificant decrease of the GUS activity with regard to the basal level. These results clearly demonstrated the capacity of OCL1 to activate the transcription of two genes of the lipid group (Table I) in the maize kernel.

In order to provide further arguments for a direct interaction between OCL1 and the regulatory region of *ZmWBC11a*, we mutated the L1 box 5′-TAA**AT**G (C/T)A-3′ to 5′-TAA**GG**G(C/T)A-3′, thereby introducing the same mutation previously used in the *PDF1* promoter to demonstrate loss of binding of the HD-ZIP IV factor ATML1 in Arabidopsis (Abe et al., 2001). We observed that in the presence of the mutated L1 box, OCL1 lost the capacity of transactivate the transcription of *ZmWBC11a* (Fig. 4C). This result demonstrated that a native L1 box was required for the transactivation by OCL1 and suggested direct binding of OCL1 to the L1 box in intron 1 of *ZmWBC11a*.

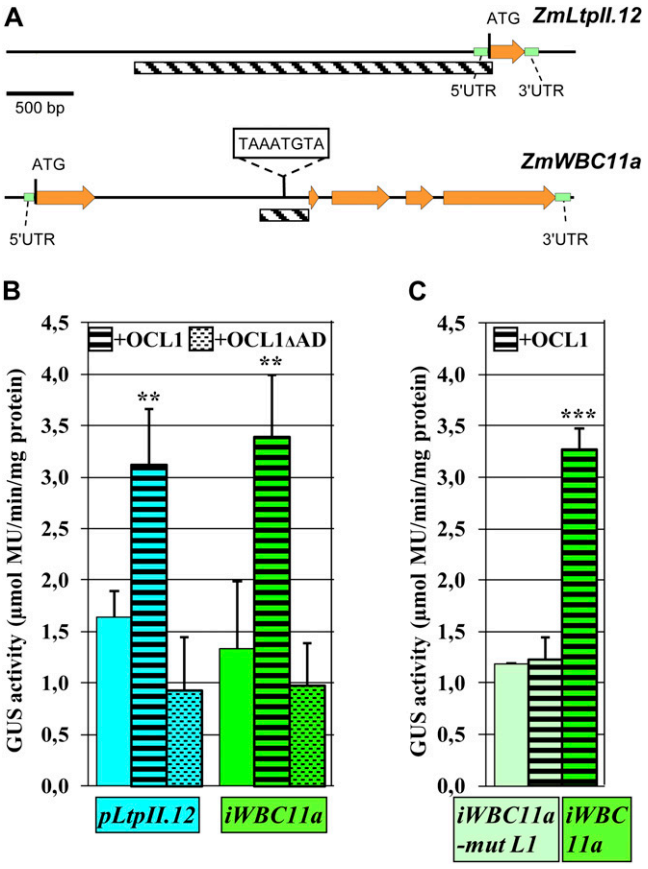

Figure 4. Transactivation of *ZmLTPII.12* and *ZmWBC11a* by OCL1 in maize kernels. A, Genomic structures of *ZmLTPII.12* and *ZmWBC11a* indicating the region fused to the *GUS* reporter gene (hatched). UTR, Untranslated region. B and C, Quantification of GUS activity from transiently transformed maize kernels. B, The reporter construct alone (no motif), with OCL1 (black stripes) or with OCL1 lacking its activation domain (AD; stippled stripes), was used for particle bombardment. C, An *iWBC11a* reporter construct mutated in the L1 box (light green) or with an intact L1 box (dark green) was used. Means and SD indicated by error bars were calculated on three biological replicates. Each replicate represented a pool of 36 bombarded kernels. ** $P < 0.01$, *** $P < 0.001$.

DISCUSSION

Transcription of 14 Genes Is Altered in Plants Overexpressing *OCL1*

The identification and molecular characterization of 14 direct or indirect target genes of the HD-ZIP IV transcription factor OCL1 showed that half of them encode proteins known to be involved in the biosynthesis or transport of cuticular waxes in maize, fitting well with the preferential or specific expression of *OCL1* in the epidermal cell layer of various plant organs. Plants overexpressing *OCL1* do not only show up-regulation of seven genes with suggestive lipid-related annotations but also alterations in the wax composition of juvenile leaves. The annotations of the remaining seven genes were less informative and

could not be readily linked to specific biological processes. The predicted localization of four gene products in the plasma membrane or cell wall hints at a role related to the cell envelope, which is not incompatible with epidermis-specific modifications. Two genes belong to the large gene families of TPR proteins and P450 cytochromes, which have been implicated in very diverse biological processes (Small and Peeters, 2000; Schuler and Werck-Reichhart, 2003); unfortunately, the position of the proteins encoded by OCL1 target genes is far from members with established functions in phylogenetic trees. The defense-related function of many P450 cytochromes provides a possible link with the last target gene *Igl*, which has previously been shown to be involved in the tritrophic defense of maize against herbivory (Frey et al., 2000).

Among the 14 genes with expression changes in *OCL1*-OE plants, eight genes showed an opposite trend in *OCL1*-RNAi knockdown lines, further supporting the hypothesis of a critical role of OCL1 in the transcriptional regulation of these target genes. The fact that a decrease in *OCL1* mRNA levels by 50% does not affect the expression level of the remaining six genes can possibly be explained either by a more complex or a less sensitive chain of events between OCL1 expression levels and target gene transcription.

OCL1 is certainly not the only regulatory protein influencing the transcription of its target genes, and it likely interacts with different proteins or via different regulatory cascades in different parts of the maize plant. These conclusions are based on the fact that the up- or down-regulation by OCL1 in seedlings is not always observed in other organs of *OCL1*-OE plants and that the expression profiles of *OCL1* and its target genes in the different organs of the maize plant overlap but do not coincide. A concrete example for independent regulation of a target gene by two different regulatory pathways is the regulation of *Igl* by volicitin (Frey et al., 2004) and OCL1. *Igl* expression was lower in *OCL1*-OE than in wild-type leaves, yet a treatment with volicitin increased *Igl* expression by a similar factor in both materials (data not shown).

OCL1 Regulates Target Genes Involved in Lipid Metabolism or Transport

Our data provide further evidence for the hypothesis that HD-ZIP IV transcription factors play important regulatory roles in the differentiation or maintenance of the epidermis in general and cuticle-related lipid metabolism and transport in particular. This hypothesis is based on the L1-specific expression pattern of most HD-ZIP IV family members on the one hand (Ariel et al., 2007) and on transcriptome data comparing epidermal cells with underlying tissues in Arabidopsis (Suh et al., 2005) and maize (Nakazono et al., 2003) on the other hand, where several *HD-ZIP IV* genes were found strongly up-regulated in epidermal tissues, just like genes involved in lipid metabolism and transport.

Here, we demonstrate the causal relationship between the overexpression of *OCL1* and the up-regulation of genes coding for a nonspecific, type 2 lipid transfer protein (nsLTPII), an AtCXE18-like carboxylesterase, a SEC14/PITP, three ABC transporters of the WBC11/ABCG11 clade, and a FAR.

Plant nsLTPs are small, soluble proteins that facilitate the transfer of fatty acids, phospholipids, glycolipids, or steroids between membranes. They are encoded by gene families with 49 and 52 members in Arabidopsis and rice, respectively (Boutrot et al., 2008). The lipid-binding capacities of the proteins and the epidermis-specific expression of many *nsLtp* genes are well documented (Kader, 1996). Roles in two distinct biological processes, defense and cuticle biosynthesis, have been demonstrated. On the one hand, overexpression of barley (*Hordeum vulgare*) LTP2 enhances tolerance to *Pseudomonas syringae* in Arabidopsis (Molina and Garcia-Olmedo, 1997), and *defective induced resistance1* mutants lack systemic acquired resistance after attack by *Pseudomonas* (Maldonado et al., 2002). On the other hand, certain *Ltp* genes can be induced by the presence of cutin monomers (Kim et al., 2008), and mutant plant lines lacking LTPG1 show a dramatic reduction of C29 alkanes (Debono et al., 2009). The two biological roles may involve a common molecular mechanism, since the *ltpG1* mutant also shows enhanced susceptibility to infection by the fungal pathogen *Alternaria brassicicola* (Lee et al., 2009). The OCL1 target *ZmLtpII.12* clusters far from *Ltp* genes with established biological functions in a phylogenetic tree, and its closest characterized neighbors are *TaLTP2* and *HvLTP2*. While no precise role has been attributed to the latter genes, there is converging evidence that *ZmLtpII.12* and consequently *OCL1* are involved in lipid transfer for cuticle biosynthesis and/or plant defense.

The second OCL1 target coding for a carboxylesterase close to AtCXE18 is also linked to both lipid metabolism and plant defense. While the biochemical function of AtCXE and related carboxylesterases (EC 3.1.1.1) is to hydrolyze esters of short-chain fatty acids (Cummins et al., 2007), a majority of carboxylesterase genes have been associated with functions in plant defense (Marshall et al., 2003).

The third lipid-related OCL1 target contains a SEC14/PITP domain named after the yeast mutant *sec14* perturbed in endosome trafficking and distinct trans-Golgi export pathways (Curwin et al., 2009). PITPs catalyze phosphatidylinositol and phosphatidylcholine transfer in vitro, and PITP deficiencies are known to be responsible for several diseases in mammals (Bankaitis et al., 2005). For example, lack of α-TOCOPHEROL TRANSFER PROTEIN causes vitamin E deficiency due to an impaired transport of α-tocopherol (Manor and Morley, 2007).

Three further OCL1 target genes involved in lipid transport are *ZmWBC11a*, *ZmWBC11b*, and *ZmWBC11c*, coding for ABC transporters of the WBC subfamily (also called ABCG subfamily), which is specialized in

the ATP-dependent translocation of steroids and other lipids in animals (Velamakanni et al., 2007). In the plant kingdom, mutant analysis has identified CER5 (WBC12) and WBC11 as key components of the cuticular lipid export pathway (Pighin et al., 2004; Bird et al., 2007). The mutants *cer5* and *wbc11* present a decrease of total cuticular wax load and varying effects on wax composition; in addition, *wbc11* presents a decrease in cutin load. While BLAST searches with entire protein sequences identified AtWBC11 as the closest relative of ZmWBC11a, a phylogenetic tree based on conserved blocks of maize, rice, and Arabidopsis sequences revealed a more complex picture (Supplemental Fig. S1). The orthologs of AtWBC11 seem to be ZmWBC11d and ZmWBC11e, which are not regulated by OCL1, while the three OCL1-controlled maize proteins ZmWBC11a, ZmWBC11b, and ZmWBC11c fell into a sister clade containing only maize and rice sequences. Nevertheless, the phylogenetic closeness to WBC11 and CER5 together with the changes in cuticular wax load observed in *OCL1*-OE plants strengthen the hypothesis that ZmWBC11a, ZmWBC11b, and ZmWBC11c are part of the cuticular lipid export pathway.

Plants Overexpressing OCL1 Show Changes in Cuticular Wax Composition

A direct link between *OCL1* and cuticle biosynthesis was established by the observation that the C24 to C28 fatty alcohol contents were significantly increased in the leaf blade and ester contents were systemically affected in the sheath and blade of *OCL1*-OE leaves. Since the decarbonylation pathway, which is responsible for the synthesis of aldehydes and alkanes, appears less affected, it seems that OCL1 expression principally affects the acyl reduction pathway. The qualitative shift in the composition of epicuticular waxes could possibly be explained by the up-regulation of the last lipid-related OCL1 target *ZmFAR1*, coding for a fatty acid reductase. Just like four other *ZmFAR* genes not regulated by OCL1, ZmFAR1 is related to CER4 (Supplemental Fig. S3). The phenotype of the *OCL1*-OE plants is somewhat complementary to the Arabidopsis *cer4* mutant, which does not accumulate C24 to C28 primary alcohols and contains intermediate levels of C30 primary alcohols (Rowland et al., 2006). More detailed comparisons between ZmFAR1 and CER4, which may accept a narrower range of substrates, are interesting but difficult, because the phylogenetic tree does not allow the identification of orthologuous gene pairs and rather establishes the existence of orthologous groups, and because the composition of cuticular waxes is quite different between maize and Arabidopsis leaves, the major compounds being C32 alcohols and aldehydes in the former but C29 and C31 alkanes in the latter case. The same limitations are valid for comparisons between the phenotypes of *OCL1*-OE plants and the Arabidopsis *wbc11* mutant, which is characterized by a significant decrease in C29 alkanes and C26 to C28 primary alcohols (Bird et al., 2007). In addition, in the WBC11 subfamily characterized by obligatory dimerization (Kusuhara and Sugiyama, 2007), the possible formation of heterodimers between ZmWBC11a, ZmWBC11b, and ZmWBC11c would further multiply the hypotheses.

A defect in fatty acid reduction has been reported in the maize double mutant *gl5/gl20*, blocked in the production of primary alcohols and showing a high accumulation of aldehydes (Bianchi et al., 1978). While *gl5* has been mapped on chromosome 4 in BIN 4.03 between markers pdi1 and umc2211, no map position is available for the duplicate locus *gl20* (http://www.maizegdb.org). However, neither *OCL1* itself nor any of the five *ZmFAR* genes mapped close to *gl5*, leaving the possibility that one of them represents *gl20*.

Transcriptional Activation Requires the OCL1 Activation Domain and an L1 Box in *ZmWBC11a*

With *ZmWBC11a*, at least one of the 14 OCL1 target genes seems to be directly activated by OCL1, since the transactivation of the *iWBC11a-GUS* reporter construct by OCL1 depends both on the presence of the activation domain in OCL1 and an intact L1 box in the 347-bp fragment of *ZmWBC11a* driving the *GUS* reporter gene. While our transactivation assays are no formal proof of physical interaction, the hypothesis of OCL1 binding to the *ZmWBC11a* L1 box is further substantiated by previous gel-shift assays or DNaseI footprints, which established in vitro physical interaction between HD-ZIP proteins and double-stranded oligonucleotides (19–21 bp) containing an L1 box for ATML1 (Abe et al., 2001), PDF2 (Abe et al., 2003), and GL2 (Ohashi et al., 2003). It is also noteworthy that the Arabidopsis *AtWBC11* contained two adjacent L1 boxes in its promoter, the shift between intron and promoter likely being the consequence of quite different intron/exon structures of *AtWBC11* and *ZmWBC11a*. Taking into account that OCL1, ATML1/PDF2, and GL2 belong to different clades of the HD-ZIP IV family and that *Helianthus annuus* homeodomain protein1 (HAHR1) interacts with an L1L box (Tron et al., 2001), our data lend further evidence to the hypothesis that the interaction between HD-ZIP proteins and an L1 or L1L box is not restricted to certain family members or to Arabidopsis but is a widespread phenomenon in the family and across species.

The transactivation of a 2,906-bp upstream fragment of *ZmLtpII.12* depended also on the presence of the activation domain in OCL1 but did not involve an L1 box, suggesting either the need for at least one additional regulatory protein in the signaling cascade between OCL1 and the *ZmLtpII.12* regulatory region or OCL1 binding to alternative sites, which may be variants of the L1 or L1L box. Preliminary results of serial promoter deletions indicate that more than 800 bp upstream of the ATG are needed for transactivation by OCL1 (data not shown). Further deletion analysis

and sequence comparisons with upstream regions and introns of the other 12 OCL1 target genes may lead to the identification of a novel cis-element recognized by an HD-ZIP IV protein and/or a yet unknown intermediary protein.

Regulation of Cuticle Biosynthesis

Cuticular wax formation is known to be tightly regulated in response to both developmental and environmental cues. Several transcription factors regulating the activity of genes involved in the synthesis of the cuticle have recently been identified. In Arabidopsis, lines overexpressing WAX INDUCER1/SHINE1 (WIN1/SHN1; Aharoni et al., 2004; Broun et al., 2004) or the closely related AP2/EREBP family members SHN2 or SHN3 (Aharoni et al., 2004) trigger wax production, enhance drought tolerance, and modulate cuticular permeability. In addition, WIN1/SHN1 overexpression also increased cutin production by the induction of cutin biosynthesis genes (Kannangara et al., 2007). Increased cuticular wax accumulation and enhanced drought tolerance were also observed by the overexpression of *M. truncatula* WAX PRODUCTION1 (WXP1), belonging to a different clade of the AP2/EREBP family, in *Medicago sativa* (Zhang et al., 2005) or Arabidopsis (Zhang et al., 2007), where the paralogous WXP2 had similar effects. The overexpression of AtMYB41, an R2R3 MYB transcription factor, led to an increased leaf epidermal permeability and modulated the expression of genes involved in lipid and cuticle metabolism (Cominelli et al., 2008). MYB30, a Myb-domain transcription factor that is induced during incompatible interactions between Arabidopsis and several bacterial pathogens (Vailleau et al., 2002), appears to positively regulate the accumulation of alkanes in cuticular waxes (Raffaele et al., 2008).

A possible link between HD-ZIP IV transcription factors and cuticle biosynthesis has previously been suggested based on coordinated up-regulation of *HD-ZIP IV* genes and genes involved in cuticle biosynthesis in the epidermal layer of Arabidopsis (Suh et al., 2005) and maize (Nakazono et al., 2003). While no cuticle defect has been described in any of the 16 *HD-ZIP IV* mutants in Arabidopsis, a point mutation in a tomato *HD-ZIP IV* gene was very recently identified as the likely cause for cutin defects of the tomato fruit in the *cd2* mutant (Isaacson et al., 2009). Phylogenetic analyses show that OCL1 falls in the same clade as CD2 and forms an orthologous group with ANL2, HDG1, HDG7, and HDG6/FLOWERING WAGENINGEN from Arabidopsis.

Our data on the regulation of lipid-related genes by OCL1 and alterations of the cuticle in *OCL1*-OE plants reinforce the hypothesis that, in addition to the above-cited members of the AP2/EREBP and MYB families, transcription factors of the HD-ZIP IV family contribute to the transcriptional regulation of cuticle biosynthesis. The presence of the START domain, which is involved in lipid binding and transport in animals (Ponting and Aravind, 1999), opens the way to the very speculative hypothesis that the activation of lipid or cuticle biosynthetic pathways by HD-ZIP IV proteins may depend on the sensing of regulatory lipids or metabolic intermediates via the START domain.

MATERIALS AND METHODS

Plant Material and Growth Conditions

The maize (*Zea mays*) inbred line A188 (Gerdes and Tracy, 1993) and transgenic A188 plants overexpressing *OCL1* were grown in a greenhouse fulfilling French S2 safety standards for the culture of transgenic plants with a 16-h illumination period (100 W m^{-2}) at 24°C/19°C (day/night) and without control of the relative humidity. Seeds were germinated in 0.2 L of Favorit MP Godets substrate (Eriterre) and were transferred at 21 DAS to 10 L of Favorit Argile TM substrate (Eriterre) supplemented with 4 g L^{-1} Osmocote Exact hi-end 15+9+12 fertilizer (Scotts). All plants were propagated by hand pollination.

T-DNA Construct and Plant Transformation

The plasmid used for the production of *OCL1*-OE and *OCL1*-RNAi plants contained the backbone of vector pSB11 (Ishida et al., 1996) and a Basta resistance cassette. For the *OCL1*-OE construct, the *OCL1* coding sequence was amplified with primers A10-6HIS5′ and A10-6HIS3′ and placed under the control of the CsVMV promoter. For the *OCL1*-RNAi construct, the inverted 350-bp *OCL1* fragments (amplified with primers OCL1-RNAi-5′ and OCL1-RNAi-3′) were separated by the rice (*Oryza sativa*) *Tubulin* intron and placed under the control of a rice *Actin* promoter followed by a rice *Actin* intron. Primer sequences are given in Supplemental Table S4.

Agrobacterium tumefaciens-mediated transformation of maize inbred line A188 was based on a published protocol (Ishida et al., 2007). Among the six independent transformation events, the two with strongest *OCL1* expression (K2 and K3) were used in this study.

Microarray Analysis

The Genoplante maize microarray contained 58,752 oligonucleotides of 70 bases spotted on glass slides. The subtending unigene set had been established by clustering the Genoplante maize EST data (http://urgi.versailles.inra.fr/data/gnpSeq/genoplante_data.php) with all publicly available EST data. Hybridization was carried out as described (Zeidler et al., 2004). Experiments were done in biological triplicate with in vitro-amplified total RNA of 18-DAS maize seedlings from wild-type and *OCL1*-OE plants. While a dye swap of the Cy5- or Cy3-labeled probes was performed, only the Cy5 data were exploited. Quantile normalization of the raw data was carried out using Spotfire software. The criteria for the inclusion of a gene in the list of differentially expressed genes were a logR > 2 or < -2 and $P < 0.01$.

qRT-PCR

Approximately 100 mg of fresh tissue was quick frozen in liquid nitrogen and ground to powder with mortar and pestle. Total RNA was extracted with 1 mL of TRIzol reagent according to the instructions of the supplier (Invitrogen). After ethanol precipitation, the RNA was resuspended in 30 μL of RNase-free water and treated with RNase-free DNase. The DNase was inactivated according to the instructions of the supplier (Ambion). Approximately 5 μg of total RNA were reverse transcribed using random hexamers (Amersham Biosciences) and reverse transcriptase without RNaseH activity (Fermentas) in a final volume of 20 μL. A total of 2.5×10^5 copies of GeneAmplimer pAW109 RNA (Applied Biosystems) were added to the RT reaction.

The cDNA was diluted 50 times, and 2 μL was used in a volume of 20 μL containing 10 μL of Platinum SYBR Green qPCR SuperMix UDG according to the instructions of the supplier (Invitrogen) to carry out qPCR on a DNA Engine Opticon 2 (Bio-Rad). Dilution series ($2n$ with $n = 0$–7) of a mixture of all cDNAs within a comparison were used to fix the threshold cycle (C_T). Gene expression levels relative to the *18S* rRNA reference gene were calculated by

the $\Delta\Delta C_T$ method (Schmittgen and Livak, 2008). The primers used are listed in Supplemental Table S4.

Sequence Analysis

The cDNA sequences corresponding to the 70mers present on the microarray were established by BLASTN individual EST sequences or full-length cDNA sequences at the National Center for Biotechnology Information (NCBI; http://www.ncbi.nlm.nih.gov/BLAST/). Consensus sequences were obtained using VectorNTI ContigExpress software (Invitrogen) and regularly updated. Genomic sequences were obtained by BLASTN of the cDNA sequence against the high-throughput genomic sequences database at NCBI. Deduced amino acid sequences were annotated by BLASTP against the Arabidopsis (*Arabidopsis thaliana*) genome at NCBI and screened for known, conserved domains using the CDS database.

Wax Composition Analysis

Maize leaf 4 sheath and blade were isolated, and their surfaces were measured by image analysis of a scan (leaf sheath was considered a cylinder for determining total surface). Cuticular waxes were extracted by immersing tissues for 30 s in 20 mL of chloroform containing 20 μg of docosane as the internal standard. Extracts were dried under a gentle stream of nitrogen, dissolved into 150 μL of BSTFA-TMCS [for *N*,*O*-bis(trimethylsilyl)trifluoroacetamide):trimethylchlorosilane (99:1)], and derivatized at 85°C for 1 h. Surplus BSTFA-TMCS was evaporated under nitrogen, and samples were dissolved in 200 μL of hexane for analysis using an Agilent 6850 gas chromatograph and helium as the carrier gas (1.5 mL min^{-1}). The gas chromatograph was programmed with an initial temperature of 80°C for 1 min and increased at 15°C min^{-1} to 260°C, held for 10 min at 200°C, increased again at 5°C min^{-1} to 320°C, and held for 15 min at 320°C. Qualitative analyses were performed using an HP-5MS column (30 m × 0.25 mm × 0.25 μm) and an Agilent 5975 mass spectrometric detector (70 eV, mass-to-charge ratio of 50–750). Quantitative analyses were performed using an HP-1 column (30 m × 0.32 mm × 0.25 μm) and a flame ionization detector. Quantification was based on peak areas and the internal standard docosane.

Laser-Capture Microdissection and RT-PCR

From the region of maximum width of fully expanded leaf 4, 1-cm^2 sections were fixed in acetone and paraffin embedded as described (Ohtsu et al., 2007). Epidermal and mesophyll subepidermal cells were microdissected from 10-μm sections using the Arcturus XT infrared laser-capture microdissection system with the following settings for epidermal/mesophyll cells, respectively: laser spot size, 10/20 μm; laser pulse duration, 20/30 ms; and laser power, 50/70 mW. About 5,000 epidermal cells (predominantly adaxial) and 2,000 mesophyll cells were collected and RNA extracted with the PicoPure RNA isolation kit (Arcturus). RNA samples were treated with DNase I (Qiagen) and amplified (two rounds) with the TargetAmpTM 2-Round aRNA Amplification kit 2.0 (Epicentre Biotechnologies). RT and PCR were carried out as described above, including a control experiment without reverse transcriptase. Primer sequences are given in Supplemental Table S4.

Transactivation Tests

The promoter regions of *ZmLtpII.12* and the first intron of *ZmWBC11a* were amplified using specific primer pairs (Supplemental Table S4). After cloning into pCRII-Blunt-Topo (Invitrogen) and sequencing, they were fused with the *GUS* reporter gene, the endogenous ATG (*ZmLtpII.12*), or an in-frame ATG in exon 2 (*ZmWBC11a*), becoming the start codon of the GUS. Plasmid DNA prepared with the PureLink HiPure Plasmid Filter Midiprep kit (Invitrogen) was used in transient transformation of 15-DAP maize kernels by particle bombardment.

The 15-DAP maize kernels were surface sterilized by pulverization of Pursept-A (Poly-Labo). The pericarp was removed in a rectangular window on the adaxial side, exposing the embryo and part of the endosperm. The kernels were plasmolyzed for 4 h on Murashige and Skoog medium (4.3 g L^{-1} MS M0221 [Duchefa], 30 g L^{-1} Suc, 0.2 g L^{-1} Asn, 36.4 g L^{-1} sorbitol, 36.4 g L^{-1} mannitol, 1 mg L^{-1} 2,4-dichlorophenoxyacetic acid, and 3 g L^{-1} Gelrite, pH 5.6) prior to bombardment.

Conditioned samples were transformed using a particle-inflow gun PDS-1000/He Biolistic Particle Delivery System (Bio-Rad). For each type of sample, the parameters were optimized according to Sanford et al. (1993). In the standard protocol, gold particles of 1 μm diameter (Bio-Rad) coated with 5 μg of plasmid DNA were propelled by helium gas under pressure (7,500 kPa) toward the samples, which were placed at 6 cm below the gun orifice. A partial vacuum (90 kPa) increased the speed of the particles. A 20-μm nylon mesh placed 3 cm above the targets protected the samples from the gas blast and dispersed the particles evenly onto them. The GUS assays were performed 48 h after transformation.

GUS Assays

Transiently transformed kernels were incubated in 5-bromo-4-chloro-3-indolyl-β-D-GlcUA for 24 h at 37°C according to Jefferson et al. (1986). Proteins were extracted with 500 μL of buffer (50 mM phosphate buffer, 10 mM EDTA, 0.1% sodium lauryl sarcosine, 0.1% Triton X-100, and 10 mM β-mercaptoethanol). The supernatant was used for quantification of GUS activity. Protein extracts were incubated with 2 mM 4-methylumbelliferyl β-D-glucuronide at 37°C during 2 h. The fluorescent product 4-methylumbelliferone (MU) was measured with a Fluoroskan II (Labsystems). Reference samples with known quantities of MU were used to determine the quantity of MU produced, which was expressed in μmol MU mg^{-1} protein min^{-1}.

Supplemental Data

The following materials are available in the online version of this article.

Supplemental Figure S1. Phylogenetic tree of maize and Arabidopsis WBC proteins.

Supplemental Figure S2. Comparison of cuticle structure in wild-type and *OCL1*-OE leaves.

Supplemental Figure S3. Phylogenetic tree of maize and Arabidopsis FAR proteins.

Supplemental Table S1. Relative expression levels of confirmed OCL1 target genes in 18-DAS plantlets.

Supplemental Table S2. Expression of 11 OCL target genes in maize organs and during kernel development as determined by qRT-PCR.

Supplemental Table S3. Composition of cuticular waxes on juvenile leaves of *OCL1*-OE and *OCL1*-RNAi plants and their wild-type siblings.

Supplemental Table S4. Primers used in this study.

ACKNOWLEDGMENTS

We thank Isabelle Anselme-Bertrand for her precious advice on electron microscopy. Isabelle Desbouchages, Alexis Lacroix, and Priscilla Angelot are acknowledged for maize culture, Hervé Leyral and Claudia Bardoux for the preparation of buffers and media, the Biogemma transcriptomics team for the hybridization and analysis of microarrays, Pierre Chambrier for advice on transient transformation, and Cédric Finet for help with phylogenetic trees. Monika Frey kindly provided us with volicitin.

Received November 5, 2009; accepted July 2, 2010; published July 6, 2010.

LITERATURE CITED

Abe M, Katsumata H, Komeda Y, Takahashi T (2003) Regulation of shoot epidermal cell differentiation by a pair of homeodomain proteins in Arabidopsis. Development **130:** 635–643

Abe M, Takahashi T, Komeda Y (2001) Identification of a cis-regulatory element for L1 layer-specific gene expression, which is targeted by an L1-specific homeodomain protein. Plant J **26:** 487–494

Aharoni A, Dixit S, Jetter R, Thoenes E, van Arkel G, Pereira A (2004) The SHINE clade of AP2 domain transcription factors activates wax biosynthesis, alters cuticle properties, and confers drought tolerance when overexpressed in *Arabidopsis*. Plant Cell **16:** 2463–2480

Ariel FD, Manavella PA, Dezar CA, Chan RL (2007) The true story of the HD-Zip family. Trends Plant Sci **12:** 419–426

Bankaitis VA, Phillips S, Yanagisawa L, Li X, Routt S, Xie Z (2005) Phosphatidylinositol transfer protein function in the yeast Saccharomyces cerevisiae. Adv Enzyme Regul **45:** 155–170

Bianchi G, Salamini F, Avato P (1978) Glossy mutants of maize. 8. Accumulation of fatty aldehydes in surface waxes of *gl5* maize seedlings. Biochem Genet **16:** 1015–1021

Bird D, Beisson F, Brigham A, Shin J, Greer S, Jetter R, Kunst L, Wu X, Yephremov A, Samuels L (2007) Characterization of Arabidopsis ABCG11/WBC11, an ATP binding cassette (ABC) transporter that is required for cuticular lipid secretion. Plant J **52:** 485–498

Boutrot F, Chantret N, Gautier MF (2008) Genome-wide analysis of the rice and Arabidopsis non-specific lipid transfer protein (nsLtp) gene families and identification of wheat nsLtp genes by EST data mining. BMC Genomics **9:** 86

Broun P, Poindexter P, Osborne E, Jiang CZ, Riechmann JL (2004) WIN1, a transcriptional activator of epidermal wax accumulation in Arabidopsis. Proc Natl Acad Sci USA **101:** 4706–4711

Cominelli E, Sala T, Calvi D, Gusmaroli G, Tonelli C (2008) Overexpression of the Arabidopsis AtMYB41 gene alters cell expansion and leaf surface permeability. Plant J **53:** 53–64

Costaglioli P, Joubes J, Garcia C, Stef M, Arveiler B, Lessire R, Garbay B (2005) Profiling candidate genes involved in wax biosynthesis in Arabidopsis thaliana by microarray analysis. Biochim Biophys Acta **1734:** 247–258

Cummins I, Landrum M, Steel PG, Edwards R (2007) Structure activity studies with xenobiotic substrates using carboxylesterases isolated from Arabidopsis thaliana. Phytochemistry **68:** 811–818

Curwin AJ, Fairn GD, McMaster CR (2009) Phospholipid transfer protein Sec14 is required for trafficking from endosomes and regulates distinct trans-Golgi export pathways. J Biol Chem **284:** 7364–7375

Debono A, Yeats TH, Rose JK, Bird D, Jetter R, Kunst L, Samuels L (2009) *Arabidopsis* LTPG is a glycosylphosphatidylinositol-anchored lipid transfer protein required for export of lipids to the plant surface. Plant Cell **21:** 1230–1238

Di Cristina M, Sessa G, Dolan L, Linstead P, Baima S, Ruberti I, Morelli G (1996) The Arabidopsis Athb-10 (GLABRA2) is an HD-Zip protein required for regulation of root hair development. Plant J **10:** 393–402

Eigenbrode SD, Espelie KE (1995) Effects of plant epicuticular lipids on insect herbivores. Annu Rev Entomol **40:** 171–194

Frey M, Spiteller D, Boland W, Gierl A (2004) Transcriptional activation of Igl, the gene for indole formation in Zea mays: a structure-activity study with elicitor-active N-acyl glutamines from insects. Phytochemistry **65:** 1047–1055

Frey M, Stettner C, Pare PW, Schmelz EA, Tumlinson JH, Gierl A (2000) An herbivore elicitor activates the gene for indole emission in maize. Proc Natl Acad Sci USA **97:** 14801–14806

Gamas P, Niebel FdeC, Lescure N, Cullimore J (1996) Use of a subtractive hybridization approach to identify new Medicago truncatula genes induced during root nodule development. Mol Plant Microbe Interact **9:** 233–242

Gerdes JT, Tracy WF (1993) Pedigree diversity within the Lancaster surecrop heterotic group of maize. Crop Sci **33:** 334–337

Glover BJ (2000) Differentiation in plant epidermal cells. J Exp Bot **51:** 497–505

Gray JE, Holroyd GH, van der Lee FM, Bahrami AR, Sijmons PC, Woodward FI, Schuch W, Hetherington AM (2000) The HIC signalling pathway links CO_2 perception to stomatal development. Nature **408:** 713–716

Guan XY, Li QJ, Shan CM, Wang S, Mao YB, Wang LJ, Chen XY (2008) The HD-Zip IV gene GaHOX1 from cotton is a functional homologue of the Arabidopsis GLABRA2. Physiol Plant **134:** 174–182

Guimil S, Dunand C (2007) Cell growth and differentiation in Arabidopsis epidermal cells. J Exp Bot **58:** 3829–3840

Ingouff M, Farbos I, Lagercrantz U, von Arnold S (2001) PaHB1 is an evolutionary conserved HD-GL2 homeobox gene expressed in the protoderm during Norway spruce embryo development. Genesis **30:** 220–230

Ingram GC, Boisnard-Lorig C, Dumas C, Rogowsky PM (2000) Expression patterns of genes encoding HD-ZipIV homeo domain proteins define specific domains in maize embryos and meristems. Plant J **22:** 401–414

Ingram GC, Magnard JL, Vergne P, Dumas C, Rogowsky PM (1999) ZmOCL1, an HDGL2 family homeobox gene, is expressed in the outer cell layer throughout maize development. Plant Mol Biol **40:** 343–354

Isaacson T, Kosma DK, Matas AJ, Buda GJ, He Y, Yu B, Pravitasari A, Batteas JD, Stark RE, Jenks MA, et al (2009) Cutin deficiency in the tomato fruit cuticle consistently affects resistance to microbial infection and biomechanical properties, but not transpirational water loss. Plant J **60:** 363–377

Ishida T, Kurata T, Okada K, Wada T (2008) A genetic regulatory network in the development of trichomes and root hairs. Annu Rev Plant Biol **59:** 365–386

Ishida Y, Hiei Y, Komari T (2007) Agrobacterium-mediated transformation of maize. Nat Protoc **2:** 1614–1621

Ishida Y, Saito H, Ohta S, Hiei Y, Komari T, Kumashiro T (1996) High efficiency transformation of maize (Zea mays L) mediated by Agrobacterium tumefaciens. Nat Biotechnol **14:** 745–750

Ito M, Sentoku N, Nishimura A, Hong SK, Sato Y, Matsuoka M (2002) Position dependent expression of GL2-type homeobox gene, Roc1: significance for protoderm differentiation and radial pattern formation in early rice embryogenesis. Plant J **29:** 497–507

Jefferson RA, Burgess SM, Hirsh D (1986) Beta-glucuronidase from Escherichia coli as a gene-fusion marker. Proc Natl Acad Sci USA **83:** 8447–8451

Jeffree CE (2006) The fine structure of the plant cuticle. *In* Biology of the Plant Cuticle, Vol 23. Blackwell Publishing, Oxford, pp 11–110

Jenks MA, Eigenbrode SD, Lemieux B (2002) Cuticular waxes of Arabidopsis. *In* C Somerville, E Meyerowitz, eds, The Arabidopsis Book, Vol 34. American Society of Plant Biologists, Rockville, MD, pp 1–22

Kader JC (1996) Lipid-transfer proteins in plants. Annu Rev Plant Physiol Plant Mol Biol **47:** 627–654

Kannangara R, Branigan C, Liu Y, Penfield T, Rao V, Mouille G, Hofte H, Pauly M, Riechmann JL, Broun P (2007) The transcription factor WIN1/SHN1 regulates cutin biosynthesis in *Arabidopsis thaliana*. Plant Cell **19:** 1278–1294

Khaled AS, Vernoud V, Ingram GC, Perez P, Sarda X, Rogowsky PM (2005) Engrailed-ZmOCL1 fusions cause a transient reduction of kernel size in maize. Plant Mol Biol **58:** 123–139

Kim TH, Park JH, Kim MC, Cho SH (2008) Cutin monomer induces expression of the rice OsLTP5 lipid transfer protein gene. J Plant Physiol **165:** 345–349

Kubo H, Peeters AJ, Aarts MG, Pereira A, Koornneef M (1999) ANTHOCYANINLESS2, a homeobox gene affecting anthocyanin distribution and root development in *Arabidopsis*. Plant Cell **11:** 1217–1226

Kunst L, Samuels AL (2003) Biosynthesis and secretion of plant cuticular wax. Prog Lipid Res **42:** 51–80

Kusuhara H, Sugiyama Y (2007) ATP-binding cassette, subfamily G (ABCG family). Pflugers Arch **453:** 735–744

Lee SB, Go YS, Bae HJ, Park JH, Cho SH, Cho HJ, Lee DS, Park OK, Hwang I, Suh MC (2009) Disruption of glycosylphosphatidylinositol-anchored lipid transfer protein gene altered cuticular lipid composition, increased plastoglobules, and enhanced susceptibility to infection by the fungal pathogen *Alternaria brassicicola*. Plant Physiol **150:** 42–54

Lu P, Porat R, Nadeau JA, O'Neill SD (1996) Identification of a meristem L1 layer-specific gene in *Arabidopsis* that is expressed during embryonic pattern formation and defines a new class of homeobox genes. Plant Cell **8:** 2155–2168

Maldonado AM, Doerner P, Dixon RA, Lamb CJ, Cameron RK (2002) A putative lipid transfer protein involved in systemic resistance signalling in Arabidopsis. Nature **419:** 399–403

Manor D, Morley S (2007) The alpha-tocopherol transfer protein. Vitam Horm **76:** 45–65

Marshall SD, Putterill JJ, Plummer KM, Newcomb RD (2003) The carboxylesterase gene family from Arabidopsis thaliana. J Mol Evol **57:** 487–500

Messing J, Dooner HK (2006) Organization and variability of the maize genome. Curr Opin Plant Biol **9:** 157–163

Molina A, Garcia-Olmedo F (1997) Enhanced tolerance to bacterial pathogens caused by the transgenic expression of barley lipid transfer protein LTP2. Plant J **12:** 669–675

Mukherjee K, Burglin TR (2006) MEKHLA, a novel domain with similarity to PAS domains, is fused to plant homeodomain-leucine zipper III proteins. Plant Physiol **140:** 1142–1150

Nadeau JA (2009) Stomatal development: new signals and fate determinants. Curr Opin Plant Biol **12:** 29–35

Nakamura M, Katsumata H, Abe M, Yabe N, Komeda Y, Yamamoto KT,

Takahashi T (2006) Characterization of the class IV homeodomain-leucine zipper gene family in Arabidopsis. Plant Physiol **141:** 1363–1375

Nakazono M, Qiu F, Borsuk LA, Schnable PS (2003) Laser-capture microdissection, a tool for the global analysis of gene expression in specific plant cell types: identification of genes expressed differentially in epidermal cells or vascular tissues of maize. Plant Cell **15:** 583–596

Nawrath C (2002) The biopolymers cutin and suberin. *In* C Somerville, E Meyerowitz, eds, The Arabidopsis Book, Vol 34. American Society of Plant Biologists, Rockville, MD, pp 1–14

Ohashi Y, Oka A, Rodrigues-Pousada R, Possenti M, Ruberti I, Morelli G, Aoyama T (2003) Modulation of phospholipid signaling by GLABRA2 in root-hair pattern formation. Science **300:** 1427–1430

Ohtsu K, Smith MB, Emrich SJ, Borsuk LA, Zhou R, Chen T, Zhang X, Timmermans MC, Beck J, Buckner B, et al (2007) Global gene expression analysis of the shoot apical meristem of maize (Zea mays L.). Plant J **52:** 391–404

Pennisi E (2008) Corn genomics pops wide open. Science **319:** 1333

Pighin JA, Zheng H, Balakshin LJ, Goodman IP, Western TL, Jetter R, Kunst L, Samuels AL (2004) Plant cuticular lipid export requires an ABC transporter. Science **306:** 702–704

Ponting CP, Aravind L (1999) START: a lipid-binding domain in StAR, HD-ZIP and signalling proteins. Trends Biochem Sci **24:** 130–132

Raffaele S, Vailleau F, Leger A, Joubes J, Miersch O, Huard C, Blee E, Mongrand S, Domergue F, Roby D (2008) A MYB transcription factor regulates very-long-chain fatty acid biosynthesis for activation of the hypersensitive cell death response in *Arabidopsis*. Plant Cell **20:** 752–767

Rerie WG, Feldmann KA, Marks MD (1994) The GLABRA2 gene encodes a homeo domain protein required for normal trichome development in Arabidopsis. Genes Dev **8:** 1388–1399

Riederer M (2006) Introduction: biology of the plant cuticle. *In* Biology of the Plant Cuticle, Vol 23. Blackwell Publishing, Oxford, pp 1–10

Rowland O, Zheng H, Hepworth SR, Lam P, Jetter R, Kunst L (2006) CER4 encodes an alcohol-forming fatty acyl-coenzyme A reductase involved in cuticular wax production in Arabidopsis. Plant Physiol **142:** 866–877

Samuels L, Kunst L, Jetter R (2008) Sealing plant surfaces: cuticular wax formation by epidermal cells. Annu Rev Plant Biol **59:** 683–707

Sanford JC, Smith FD, Russell JA (1993) Optimizing the biolistic process for different biological applications. Methods Enzymol **217:** 483–509

Schmittgen TD, Livak KJ (2008) Analyzing real-time PCR data by the comparative C(T) method. Nat Protoc **3:** 1101–1108

Schuler MA, Werck-Reichhart D (2003) Functional genomics of P450s. Annu Rev Plant Biol **54:** 629–667

Shen B, Sinkevicius KW, Selinger DA, Tarczynski MC (2006) The homeobox gene GLABRA2 affects seed oil content in Arabidopsis. Plant Mol Biol **60:** 377–387

Sieburth LE, Meyerowitz EM (1997) Molecular dissection of the AGAMOUS control region shows that cis elements for spatial regulation are located intragenically. Plant Cell **9:** 355–365

Small ID, Peeters N (2000) The PPR motif: a TPR-related motif prevalent in plant organellar proteins. Trends Biochem Sci **25:** 46–47

Suh MC, Samuels AL, Jetter R, Kunst L, Pollard M, Ohlrogge J, Beisson F (2005) Cuticular lipid composition, surface structure, and gene expression in Arabidopsis stem epidermis. Plant Physiol **139:** 1649–1665

Tominaga-Wada R, Iwata M, Sugiyama J, Kotake T, Ishida T, Yokoyama R, Nishitani K, Okada K, Wada T (2009) The GLABRA2 homeodomain protein directly regulates CESA5 and XTH17 gene expression in Arabidopsis roots. Plant J **60:** 564–574

Tron AE, Bertoncini CW, Palena CM, Chan RL, Gonzalez DH (2001) Combinatorial interactions of two amino acids with a single base pair define target site specificity in plant dimeric homeodomain proteins. Nucleic Acids Res **29:** 4866–4872

Vailleau F, Daniel X, Tronchet M, Montillet JL, Triantaphylides C, Roby D (2002) A R2R3-MYB gene, AtMYB30, acts as a positive regulator of the hypersensitive cell death program in plants in response to pathogen attack. Proc Natl Acad Sci USA **99:** 10179–10184

Velamakanni S, Wei SL, Janvilisri T, van Veen HW (2007) ABCG transporters: structure, substrate specificities and physiological roles. A brief overview. J Bioenerg Biomembr **39:** 465–471

Vernoud V, Laigle G, Rozier F, Meeley RB, Perez P, Rogowsky PM (2009) The HD-ZIP IV transcription factor OCL4 is necessary for trichome patterning and anther development in maize. Plant J **59:** 883–894

Zeidler M, Zhou Q, Sarda X, Yau CP, Chua NH (2004) The nuclear localization signal and the C-terminal region of FHY1 are required for transmission of phytochrome A signals. Plant J **40:** 355–365

Zhang JY, Broeckling CD, Blancaflor EB, Sledge MK, Sumner LW, Wang ZY (2005) Overexpression of WXP1, a putative Medicago truncatula AP2 domain-containing transcription factor gene, increases cuticular wax accumulation and enhances drought tolerance in transgenic alfalfa (Medicago sativa). Plant J **42:** 689–707

Zhang JY, Broeckling CD, Sumner LW, Wang ZY (2007) Heterologous expression of two Medicago truncatula putative ERF transcription factor genes, WXP1 and WXP2, in Arabidopsis led to increased leaf wax accumulation and improved drought tolerance, but differential response in freezing tolerance. Plant Mol Biol **64:** 265–278

Fig. S1 Javelle et al.

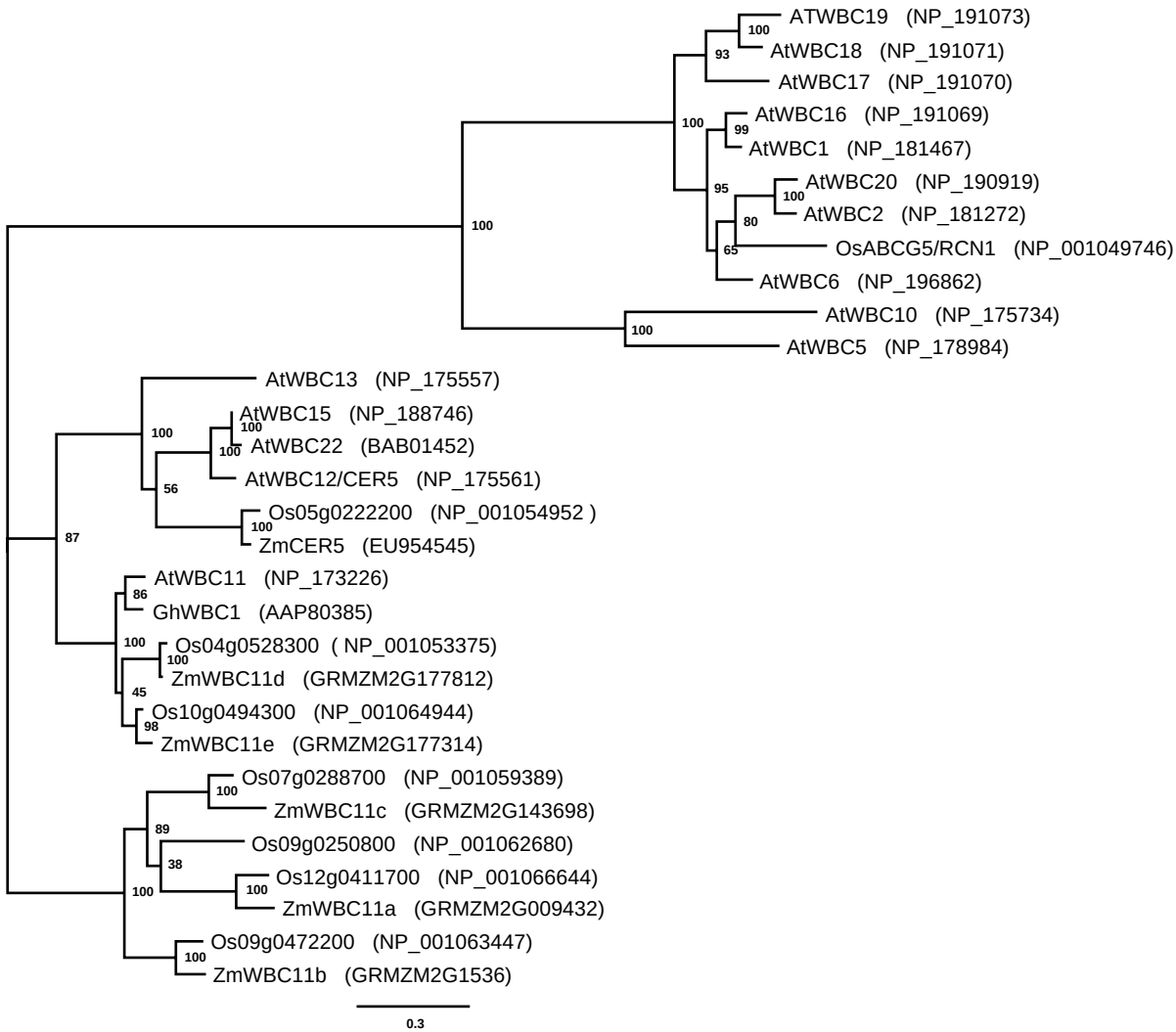

Fig. S1: Phylogenetic tree of maize and *Arabidopsis thaliana WBC* genes

Maximum likelihood phylogenetic trees were generated using all WBC amino acid sequences available in the *Arabidopsis thaliana* and maize genomes. Amino acid sequences were aligned by ClustalW. Conserved blocks were selected manually with the Seaview program (http://pbil.univ-lyon1.fr/software/seaview.html) and phylogenetic trees were generated from these selected aligned blocks using Treefinder software (www.treefinder.de) with the substitution model WAG_optimumG4 and 1000 bootstraps replicates. Percentage values on each branch represent the corresponding bootstrap probability.

Fig. S2 Javelle et al.

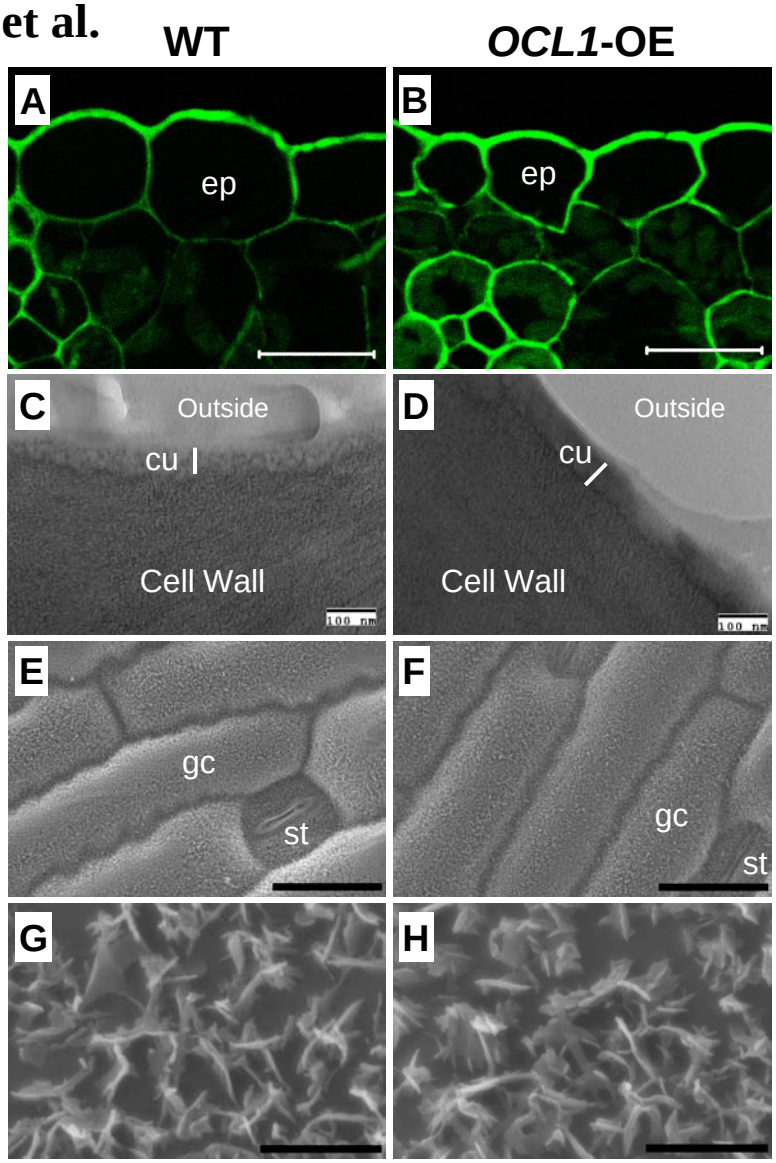

Fig. S2: Comparison of cuticle structure in wild-type and *OCL1*-OE leaves

Transverse sections of juvenile leaves (leaf #4) of wild-type (A and C) or *OCL1*-OE (B and D) were stained with auramine O (A and B) or observed in a transmission electron microscope (C and D). Epicuticular wax crystals of wildtype (E and G) or *OCL1*-OE (F and H) leaf #4 were observed in a scanning electron microscope (E to H). cu, cuticle; ep, epidermal cell; gc, ground cell; st, stomata. Scale bars, 20 µm in A and B; 100 nm in C and D; 30 µm in E and F; 2 µm in G and H.

Auramine O staining was adapted from two published protocols (Heslop-Harrison, 1997, Ann Bot 41:913-922; Lequeu et al., 2003, Plant J 36:155-164). Maize leaf samples were infiltrated under vacuum in 2% glutaraldehyde, 2% para-formaldehyde and 0.3% Tween20 for two times 10 min. Fixation was pursued overnight at 4°C in fresh fixative. Samples were dehydrated in an ethanol series and embedded in Technovit 7100 resin (Hereaus Kulzer) according to the manufacturer's instructions. Transverse sections of 4 µm were collected on glass slides and stained for 10 min in 0.01% Auramine O in 50 mM Tris pH 7.2 (Sigma).

Tissue preparation for TEM analysis was done according to Ma et al. (2008, Planta, 227:527-538), except that samples were embedded in hard LV Agar resin (Agar Scientific, Saclay, France). Ultrathin sections of 60-80 nm were cut on a Leica RMC MTXL ultramicrotome with a diamond knife and lifted onto 300-mesh copper grids. Grids were stained in 2% uranyl-acetate and lead-citrate and observed on a Hitachi H-800 transmission electronic microscope.

Fig. S3 Javelle et al.

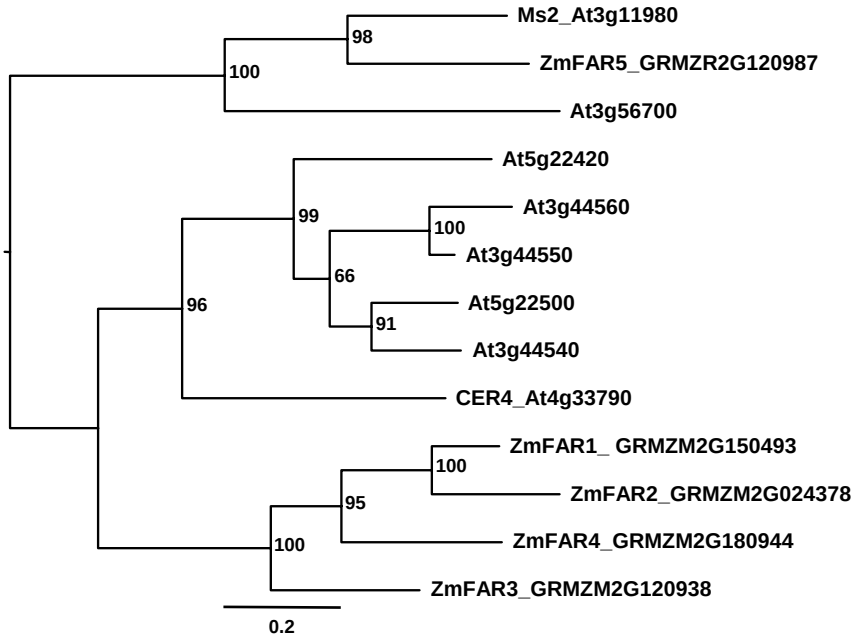

Fig. S3: Phylogenic tree of maize and *Arabidopsis thaliana* FAR proteins
Maximum likelihood phylogenetic trees were generated using all FAR amino acid sequences available in the *Arabidopsis thaliana* and maize genomes. Amino acid sequences were aligned by ClustalW. Conserved blocks were selected manually with the Seaview program (http://pbil.univ-lyon1.fr/software/seaview.html) and phylogenetic trees were generated from these selected aligned blocks using Treefinder software (www.treefinder.de) with the substitution model WAG_optimumG4 and 1000 bootstraps replicates. Percentage values on each branch represent the corresponding bootstrap probability.

Table S1: Relative expression levels of confirmed OCL1 target genes in 18 DAS plantlets

Oligo ID[1] or gene name	Trend in *OCL1*-OE	Mean[2] *OCL1*-OE	SD[3] *OCL1*-OE	Mean[2] WT	SD[3] WT	P-value Student test	Ratio *OCL1*-OE / WT
OCL1	Up	21.18	3.75	0.89	0.12	0.00036	23.80
MZ00005958	Down	0.15	0.02	0.85	0.16	0.000794	0.18
MZ00014373	Down	0.11	0.01	1.19	0.30	0.001651	0.10
MZ00018561	Down	0.29	0.13	0.77	0.21	0.01355	0.38
MZ00022171	Up	27.07	7.22	1.30	0.98	0.001795	20.88
MZ00024305 *ZmLtpII.12*	Up	4.58	0.21	1.06	0.23	0.00002	4.34
MZ00024414	Down	0.08	0.02	0.94	0.06	0.000011	0.09
MZ00028617	Down	0.03	0.01	0.89	0.09	0.000046	0.04
MZ00029574	Up	6.64	0.36	0.90	0.15	0.000007	7.35
MZ00030315	Up	13.42	1.25	0.99	0.15	0.000035	13.51
MZ00031783 *ZmWBC11a*	Up	6.43	0.14	0.93	0.24	0.000002	6.94
MZ00031955	Up	8.59	0.72	1.21	0.34	0.000044	7.08
ZmFAR1	Up	2.32	0.51	0.83	0.23	0.007236	2.78
ZmWBC11b	Up	2.76	0.41	1.02	0.18	0.001268	2.69
ZmWBC11c	Up	2.12	0.11	1.03	0.03	0.000041	2.06

[1] Identification number of the corresponding oligonucleotide deposited on the micro-array

[2] Mean of a biological triplicate and technical replicate; the relative expression values were reported to one of the WT samples

[3] Standard deviation calculated on biological triplicate

Table S2: Expression of 11 OCL target genes in maize organs and during kernel development as determined by qRT-PCR[1]

Oligo ID[2] or gene name	juvenile leaf blade	juvenile leaf sheath	adult leaf blade	adult leaf sheath	root 7 DAS	root 30 DAS	aerial parts seed-ling	imma-ture ear	mature ear	imma-ture tassel	mature tassel	silk	stem	kernel 12 DAP	pollen	shoot apex	imma-ture ovule	mature ovule	01 DAP	03 DAP	05 DAP	07 DAP	09 DAP	12 DAP	15 DAP	20 DAP	30 DAP	35 DAP	50 DAP	70 DAP
MZ00028491 (*OCL1*)	2.00	0.92	1.62	0.47	1.25	0.80	3.68	11.04	6.12	6.68	0.91	4.27	0.06	0.57	0.00	7.46	2.39	3.13	2.12	2.17	1.24	2.30	1.80	1.58	0.09	0.13	1.04	0.57	0.69	0.81
MZ00005958	49.46	4.16	0.61	0.05	0.33	5.40	22.44	0.10	1.33	0.13	21.31	3.56	0.41	0.19	0.06	0.64	0.73	0.76	1.20	0.69	0.23	13.07	1.87	0.54	0.00	0.54	2.84	3.38	0.60	0.23
MZ00014373	7.66	3.96	8.49	3.26	5.03	0.39	3.83	0.02	1.08	0.03	1.39	0.00	4.73	0.00	0.00	0.04	14.61	8.16	2.26	0.73	1.03	7.18	1.20	0.28	0.02	0.05	1.13	1.94	2.40	0.40
MZ00018561	0.00	0.00	0.00	0.00	0.00	0.00	0.00	0.78	1.77	0.61	1.17	0.00	0.00	0.00	0.00	0.00	0.00	0.00	0.00	0.00	0.00	0.00	0.00	0.00	0.00	0.00	0.00	0.00	0.00	0.00
MZ00022171	0.59	0.23	0.21	0.27	0.89	1.14	9.03	0.69	7.31	0.43	0.50	4.70	0.20	80.12	0.14	1.23	0.25	0.64	0.49	0.31	0.23	1.90	3.11	5.12	1.75	3.80	1.89	2.47	0.52	0.36
MZ00024305 (*ZmLtpII.12*)	3.73	24.58	0.33	49.51	2.03	0.05	9.58	0.02	0.86	1.24	184.14	0.09	0.22	5.28	0.09	0.02	0.70	1.26	0.81	3.38	41.42	25.58	3.57	4.10	0.67	0.08	0.18	0.18	0.08	0.19
MZ00024414	4.48	0.08	6.37	0.06	3.74	0.63	34.83	2.27	0.27	1.15	0.96	0.06	0.00	2.86	0.00	0.85	0.00	0.69	0.39	0.01	0.98	9.47	143.85	172.26	9.44	3.77	0.31	6.84	0.00	0.00
MZ00028617	10.54	12.15	81.70	61.28	0.02	0.18	0.04	0.55	1.75	0.78	0.08	0.27	8.68	0.21	0.00	0.45	0.51	0.48	0.28	0.62	0.10	1.11	1.09	4.08	0.43	0.50	7.35	7.80	3.12	1.23
MZ00029574	0.31	15.48	0.25	0.99	0.38	0.54	10.57	0.64	0.36	0.18	48.73	0.53	0.50	0.12	19.79	0.32	0.00	0.00	0.29	0.04	0.97	11.90	0.60	0.00	0.00	0.00	4.99	2.71	0.00	0.00
MZ00030315	68.70	5.02	23.14	4.86	1.67	1.34	0.24	0.01	0.07	0.67	8.77	0.30	2.97	0.29	0.07	0.00	0.00	0.00	0.00	0.00	0.00	11.92	2.56	0.66	0.47	0.46	3.62	0.70	0.24	0.38
MZ00031783 (*ZmWBC11a*)	3.11	6.58	1.42	1.54	0.07	0.12	3.12	0.66	20.01	0.76	32.84	54.47	0.11	0.60	0.00	0.38	1.11	1.95	1.00	0.67	0.70	4.02	4.65	4.03	0.39	0.34	1.41	0.64	0.70	0.16
MZ00031955	0.44	0.98	0.44	0.50	0.00	0.00	3.16	2.39	4.14	2.85	1.42	10.88	0.21	0.12	0.00	0.31	0.93	1.60	1.00	0.35	0.73	2.58	2.39	1.61	0.34	0.40	0.76	2.77	2.69	0.34

[1] Relative expression levels normalised with the *18S* RNA gene as described in materials and methods (means of a technical replicate)

[2] Identification number of the corresponding oligonucleotide deposited on the micro-array

Table S3: Composition of cuticular waxes on juveniles leaves of *OCL1*-OE and *OCL1*-RNAi plants and their wildtype siblings

Leaf blade		OCL1-OE (event K2)					OCL1-OE (event K3)					OCL1-RNAi (line 1)					OCL1-RNAi (line 2)					OCL1-RNAi (line 3)				
µg/cm2	Chain length	WT		*OCL1*-OE		Significance[1]	WT		*OCL1*-OE		Significance[1]	WT		*OCL1*-RNAi		Significance[1]	WT		*OCL1*-RNAi		Significance[1]	WT		*OCL1*-RNAi		Significance[1]
		Mean	SD	Mean	SD		Mean	SD	Mean	SD		Mean	SD	Mean	SD		Mean	SD	Mean	SD		Mean	SD	Mean	SD	
Alkanes	C25	0,018	0,005	0,025	0,005	**	0,016	0,003	0,025	0,007	**	0,025	0,007	0,026	0,005		0,036	0,019	0,025	0,006		0,029	0,005	0,021	0,004	
	C27	0,034	0,018	0,043	0,020		0,025	0,009	0,035	0,012		0,045	0,016	0,044	0,009		0,055	0,020	0,047	0,017		0,063	0,009	0,048	0,005	
	C29	0,059	0,024	0,072	0,025		0,052	0,009	0,055	0,009		0,055	0,012	0,055	0,013		0,058	0,012	0,066	0,008		0,066	0,008	0,060	0,006	
	C31	0,150	0,014	0,151	0,030		0,156	0,013	0,146	0,021		0,159	0,028	0,169	0,037		0,187	0,036	0,217	0,037		0,207	0,033	0,216	0,017	
	C33	0,083	0,013	0,089	0,011		0,092	0,012	0,095	0,016		0,087	0,018	0,085	0,017		0,132	0,030	0,146	0,028		0,161	0,051	0,155	0,012	
Alcohols	C24	0,030	0,007	0,048	0,009	**	0,036	0,008	0,054	0,012	**	0,039	0,010	0,036	0,012		0,037	0,012	0,023	0,006		0,018	0,005	0,017	0,003	
	C26	0,027	0,011	0,058	0,010	**	0,027	0,007	0,041	0,010	**	0,020	0,005	0,018	0,006		0,015	0,004	0,014	0,007		0,011	0,003	0,008	0,002	
	C28	0,025	0,008	0,043	0,004	**	0,022	0,007	0,040	0,008	**	0,042	0,009	0,041	0,013		0,029	0,011	0,038	0,009		0,034	0,009	0,027	0,006	
	C30	0,171	0,025	0,207	0,015	**	0,189	0,019	0,198	0,039		0,148	0,029	0,143	0,032		0,100	0,021	0,106	0,018		0,061	0,014	0,077	0,007	*
	C32	5,368	0,523	4,887	0,517		5,574	0,510	4,837	1,048		4,316	0,771	3,934	0,926		4,091	0,326	3,758	0,574		3,219	0,436	3,578	0,368	
Esters	C40	0,040	0,006	0,033	0,010		0,038	0,012	0,041	0,009	**	0,040	0,010	0,037	0,012		0,037	0,007	0,035	0,009		0,054	0,016	0,034	0,010	*
	C42	0,047	0,010	0,035	0,013		0,046	0,013	0,036	0,010		0,040	0,011	0,033	0,012		0,038	0,015	0,024	0,006	*	0,056	0,028	0,031	0,013	
	C44	0,055	0,010	0,041	0,016		0,054	0,016	0,037	0,011		0,043	0,010	0,028	0,012	*	0,032	0,008	0,020	0,007	*	0,029	0,010	0,019	0,006	
	C46	0,032	0,006	0,022	0,008	**	0,030	0,009	0,015	0,005	**	0,019	0,005	0,009	0,005	**	0,011	0,003	0,004	0,003	**	0,007	0,001	0,004	0,001	**
	C48	0,023	0,005	0,014	0,004	**	0,024	0,007	0,012	0,004	**	0,012	0,003	0,006	0,003	**	0,007	0,001	0,002	0,002	**	0,004	0,001	0,002	0,001	*
Aldehyde	C28	0,018	0,004	0,028	0,003	**	0,018	0,003	0,021	0,004		0,014	0,003	0,014	0,003		0,013	0,003	0,013	0,001		0,011	0,002	0,010	0,001	
	C30	0,138	0,036	0,178	0,022	**	0,146	0,019	0,158	0,029		0,151	0,036	0,159	0,034		0,139	0,034	0,163	0,020		0,165	0,022	0,147	0,013	
	C32	1,852	0,180	1,691	0,303		1,853	0,170	1,772	0,386		1,843	0,523	1,975	0,339		1,888	0,261	1,830	0,228		1,701	0,394	1,712	0,177	
Total wax load		8,329	0,665	7,782	0,764		8,557	0,717	7,735	1,578		8,440	1,710	8,141	1,641		8,561	0,635	8,183	0,852		7,519	0,990	7,574	0,625	

[1] * indicates p-value < 0.05; ** indicates p-value < 0.01 in Student's t-test

Leaf Sheath		OCL1-OE (event K2)					OCL1-OE (event K3)					OCL1-RNAi (line 1)					OCL1-RNAi (line 2)					OCL1-RNAi (line 3)				
µg/cm2	Chain length	WT		*OCL1*-OE		Significance[1]	WT		*OCL1*-OE		Significance[1]	WT		*OCL1*-RNAi		Significance[1]	WT		*OCL1*-RNAi		Significance[1]	WT		*OCL1*-RNAi		Significance[1]
		Mean	SD	Mean	SD		Mean	SD	Mean	SD		Mean	SD	Mean	SD		Mean	SD	Mean	SD		Mean	SD	Mean	SD	
Alkanes	C25	0,084	0,022	0,102	0,032		0,064	0,027	0,083	0,042		0,024	0,005	0,023	0,004		0,031	0,00646	0,03526	0,01175		0,023	0,00388	0,026614	0,008817	
	C27	0,119	0,033	0,175	0,071	*	0,086	0,026	0,124	0,052		0,040	0,004	0,039	0,012		0,048	0,01342	0,05532	0,0249		0,042	0,01043	0,043905	0,025384	
	C29	0,143	0,047	0,170	0,053		0,117	0,048	0,134	0,040		0,057	0,011	0,054	0,009		0,062	0,01055	0,09425	0,04327		0,059	0,00691	0,060602	0,014247	
	C31	0,169	0,027	0,171	0,041		0,169	0,047	0,142	0,016		0,052	0,014	0,050	0,006		0,055	0,01601	0,08963	0,05605		0,065	0,00905	0,056853	0,015038	
	C33	0,105	0,012	0,128	0,029	*	0,102	0,032	0,131	0,026		0,016	0,003	0,017	0,002		0,019	0,00508	0,04981	0,06229		0,020	0,00586	0,018926	0,004923	
Alcohols	C24	0,046	0,031	0,064	0,033		0,061	0,025	0,081	0,040		0,026	0,005	0,028	0,009		0,037	0,01604	0,02799	0,00815		0,021	0,00913	0,019931	0,006887	
	C26	0,027	0,005	0,043	0,020	*	0,023	0,013	0,029	0,014		0,016	0,005	0,014	0,003		0,023	0,00683	0,03031	0,02604		0,014	0,00155	0,017538	0,008659	
	C28	0,075	0,019	0,066	0,038		0,062	0,023	0,059	0,012		0,009	0,002	0,007	0,002		0,015	0,00409	0,02713	0,02729		0,009	0,00144	0,010062	0,003664	
	C30	0,073	0,019	0,084	0,022		0,065	0,018	0,084	0,026		0,076	0,011	0,072	0,010		0,089	0,02314	0,1057	0,01917		0,081	0,0124	0,077448	0,012558	
	C32	1,498	0,232	1,773	0,278	*	1,441	0,319	1,927	0,511	*	0,021	0,003	0,022	0,002		0,031	0,00707	0,03454	0,01428		0,024	0,0037	0,026135	0,004229	
Esters	C40	0,047	0,017	0,073	0,034	*	0,045	0,026	0,053	0,026		0,049	0,005	0,053	0,006		0,062	0,01282	0,08363	0,054		0,057	0,00748	0,055301	0,010	
	C42	0,081	0,010	0,078	0,031		0,043	0,013	0,071	0,050		0,065	0,011	0,072	0,015		0,089	0,02317	0,12536	0,093		0,077	0,0168	0,073406	0,016	
	C44	0,046	0,007	0,095	0,040	**	0,042	0,011	0,117	0,057	**	0,062	0,021	0,067	0,018		0,078	0,01725	0,11279	0,09121		0,070	0,01898	0,067383	0,01539	
	C46	0,033	0,008	0,081	0,027	**	0,032	0,007	0,091	0,038	**	0,025	0,010	0,024	0,006		0,029	0,00742	0,0406	0,02987		0,025	0,00713	0,023572	0,006306	
	C48	0,026	0,007	0,070	0,022	**	0,023	0,004	0,083	0,034	**	0,007	0,001	0,004	0,001		0,008	0,0022	0,02023	0,02706		0,007	0,00164	0,007877	0,003214	
Aldehyde	C28	0,020	0,003	0,024	0,011		0,017	0,008	0,022	0,008		0,032	0,009	0,030	0,004	**	0,031	0,01074	0,04887	0,03335		0,042	0,00715	0,037184	0,009615	
	C30	0,176	0,046	0,181	0,052		0,163	0,052	0,173	0,041		0,035	0,010	0,035	0,008		0,036	0,01483	0,04831	0,01903		0,059	0,01327	0,055608	0,021681	
	C32	1,694	0,351	1,320	0,241	*	1,825	0,381	1,214	0,262	**	0,022	0,008	0,023	0,005		0,022	0,00637	0,0467	0,04487		0,049	0,0526	0,028879	0,006789	
Total wax load		4,598	0,662	4,988	0,749		4,515	0,839	4,746	0,973		5,830	0,940	6,045	0,509		6,759	0,95547	7,46269	1,26948		7,204	0,96979	6,778214	0,905827	

[1] * indicates p-value < 0.05; ** indicates p-value < 0.01 in Student's t-test

Table S4: Primers used in this study

Oligo ID[1] or gene name	Primer sequence (5' to 3')	Primer name	Use
OCL1 *MZ00028491*	GCCTGTGGGCTATGTATCCG	OCL1sp-1298F	Expression *OCL1*-OE/WT
	GTGGCCTTAGCAATCATGCAC	OCL1sp-1432R	
	ATGCAGCTCGTCATGAACG	OCL1-2370F	RT-PCR on LCM samples
	CAGAATATGAGGTTGTTCACGG	OCL1-2581R	
MZ00005958	TGGTAGCGCAATGGTGAGACA	OCL1_down17-328F	Expression *OCL1*-OE/WT
	CGTGCTTGCTAACACAGCCTATAT	OCL1_down17-478R	
MZ00014373	CATATGCTCATGACCAGTCCGT	OCL1_down3-145F	Expression *OCL1*-OE/WT
	CGCGCTTCCAAACATCCTT	OCL1_down3-515R	
MZ00018561	GTTAACGAGTGCGGCAAGCAT	OCL1_down21-442F	Expression *OCL1*-OE/WT
	GCGTGTATAACTTTGACCGCGTAT	OCL1_down21-606R	
MZ00022171	AAATTCGGCACACACTCGACTC	OCL1_UP5-9F	Expression *OCL1*-OE/WT
	AAGATCGTCCGGAAAGTGGAGG	OCL1_UP5-301R	
	ATCAGTAGCAGCAGCATCTT	UP5-F2	RT-PCR on LCM samples
	CATCAAGCACATACACGACT	UP5-R2	
ZmLtpII.12 *MZ00024305*	CCTCGTGGTGTGGATGAATAA	UP2-3232F couple n°6	Expression *OCL1*-OE/WT
	CATGACACAACCGCTCTTGGTAA	UP2-3484R couple n°6	
MZ00024414	GCTCTGTCGTCTTCAAATCCGC	OCL1_down9-173F	Expression *OCL1*-OE/WT
	ACATAGTTGGTGTTCCCCTCGG	OCL1_down9-373R	
	ACTGCAAGGGTGGATGGATG	Down9-F1	RT-PCR on LCM samples
	GGTGACAATGGTGAAGCCAT	Down9-R1	
MZ00028617	AAGCGGTTCAGAAGTCGGTTG	OCL1_down12-238F	Expression *OCL1*-OE/WT
	TTCGGCACCTGATCGATACAC	OCL1_down12-407R	
MZ00029574	CTGCGCAGATATAGCACTTCTTCAC	OCL1_UP6-25F	Expression *OCL1*-OE/WT
	AAGGCCTCTGGTTCCGACTAGA	OCL1_UP6-231R	
MZ00030315	CCGCTCACGCTCTACATTGTT	OCL1_UP1-144F	Expression *OCL1*-OE/WT
	AAGTTCTGCCGTCACATTGGC	OCL1_UP1-364R	
ZmWBC11a *MZ00031783*	TCCATACCTGTCCGTCGTTTCC	OCL1_UP3-264F	Expression *OCL1*-OE/WT
	TTGAGCATCATGACACCCTGC	OCL1_UP3-479R	
	TGATGCTGGTGTACAGGATG	UP3-F1	RT-PCR on LCM samples
	TTGTGGTCGGTTGTCTATCC	UP3-R1	
MZ00031955	GAAGTTTCTCGTTGTCTTCG	OCL1_UP4-252F	Expression *OCL1*-OE/WT
	GTGTACAACGACAGTTCGGA	OCL1_UP4-467R	
	ATAATGGCGAGGCCACCTCTT	UP4-F1	RT-PCR on LCM samples
	GTGGCTCAGAGCATATACAG	UP4-R1	
ZmFAR1	TACCTGTTCTATGGATCGACCG	ZmCER4-1945F	Expression *OCL1*-OE/WT
	GCCACCTAACACAGCATACACTC	ZmCER4-2095R	
ZmWBC11b	ACGCTGGTGAACTCGTACAAAG	ZmWBC11b3520F	Expression *OCL1*-OE/WT
	AGGAAACTTGCCTGCCATTC	ZmWBC11b3635R	
ZmWBC11c	CTTGTGGAAGTACCCGACGTAC	ZmWBC11c6812F	Expression *OCL1*-OE/WT
	GCCCCTTTCCTAACACACCAT	ZmWBC11c6924R	
ZmWBC11d	ACATCGCGAGGAAGAGGAT	ZmWBC11d2240F	Expression *OCL1*-OE/WT
	CAATATAACACCAAGAGCCGG	ZmWBC11d2423R	
ZmWBC11e	GCCGATGCGCAACCCG	ZmWBC11e3803F	Expression *OCL1*-OE/WT
	CATCGCTTCCGACGTCGTC	ZmWBC11e3953R	
OCL1-6His	GCTCCCGGGATGAGCTTCGGGAGCCTATTCGAC	A10-6HIS5'	*OCL1*–OE construct
	GCTCCCGGGTCAATGGTGATGGTGATGATGAGCGTC	A10-6HIS3'	
OCL1	GCACCTGTGCATCGAGAATGCGC	OCL1-RNAi-5'	*OCL1*-RNAi construct
	CTAGTTCATCCATGGCGCTGATC	OCL1-RNAi-3'	
LtpII.12 promoter	TTTCACCCGGGAGACTGCGTG	OCL1_UP2-promF	*Trans*-activation
	CTCGCCATGGGCACTAACTAGCTT	OCL1_UP2-ATG-R	
ZmWBC11a intron	CGGGCACTCGAGTAGTGTATAGTCA	UP3gXho-62F	*Trans*-activation
	GTTTTATCCATGGCGGGTCCTAA	UP3gNco-427R	

[1] Identification number of the corresponding oligonucleotide deposited on the micro-array